The Ballast Effect of Lithogenic Matter and its Influences on the Carbon Fluxes in the Indian Ocean

Tim Rixen[1,2], Birgit Gaye[2], Kay-Christian Emeis[2,3], Venkitasubramani Ramaswamy[4]

[1]Leibniz Center for Tropical Marine Research, Bremen, 28359, Germany
[2] Institute of Geology, University of Hamburg, Hamburg, 20146, Germany
[3]Helmholtz-Zentrum Geesthacht, Institute of Coastal Research, Geesthacht, 21502, Germany
[4] National Institute of Oceanography, Dona Paula, Goa, 403004, India

Correspondence to: Tim Rixen (Tim.Rixen@leibniz-zmt.de)

Abstract. Data obtained from long-term sediment trap experiments in the Indian Ocean were analysed in conjunction with satellite-derived observations to study the influence of primary production and the ballast effect on organic carbon flux into the deep sea. Our results suggest that primary production mainly controlled the spatial variability of carbonate and organic carbon fluxes at our study sites in the open Indian Ocean. At trap sites in the river-influenced northern and central Bay of Bengal and off South Java lithogenic matter was the main ballast material and its content strongly influenced organic carbon fluxes favoured by weakly pronounced variability of primary production at our trap locations in these regions. Densities of ballast minerals were compiled from the literature and used in addition to their fluxes measured by sediment traps and satellite-derived export production rates, to calculate sinking speeds and organic carbon fluxes. These calculations imply that lithogenic matter could increase the mean sinking speeds by 34% and the mean calculated organic carbon flux by 41% at sites in the open Indian Ocean due to the effect of sinking speeds on organic carbon flux. At trap locations in the river-influenced regions of the Indian Ocean an enhanced lithogenic matter content and a resulting stronger ballast effect increased the calculated organic carbon fluxes by up to 62%. This explains high measured organic carbon fluxes in the low-productive South Java Sea, which exceeded those determined in the highly productive western Arabian Sea. The strong effect of lithogenic matter on the organic carbon flux as seen at the study sites in the Indian Ocean implies that land use changes and the associated transport of lithogenic matter from land into the ocean effects the CO_2 uptake of organic carbon pump significantly.

1 Introduction

Photosynthesis and the export of organic matter from the euphotic zone into the deep sea drives the organic carbon pump and is an integral part of the global carbon cycle (Volk and Hoffert, 1985). The amount of nutrients used to fix CO_2 strongly influences the CO_2 uptake of the organic carbon pump. At present, phytoplankton utilises about half of the nutrients stored in

the ocean. These nutrients are called regenerated nutrients and the CO_2 associated with them is called regenerated CO_2. The other half of the nutrients stored in the ocean eludes its utilisation and remains biologically unused (Duteil et al., 2012; Ito and Follows, 2005; Knox and McElroy, 1984; Sarmiento and Toggweiler, 1984; Siegenthaler and Wenk, 1984). These so-called 'preformed nutrients' (Broecker et al., 1985) originate at higher latitudes when upwelling and convective mixing introduce regenerated nutrients and CO_2 into the surface layer and light limitation prevents their photosynthetic assimilation in winter. Whereas regenerated CO_2 returns into the atmosphere, convective mixing and subduction of denser polar water beneath the warmer and lighter subtropical water masses restores former regenerated nutrients as preformed nutrients into the deep ocean. The lower the preformed nutrients formation rate the higher the amount of regenerated nutrients and CO_2 stored by the organic carbon pump in the ocean (e.g., Ito and Follows, 2005). The ratio between total (regenerated and preformed) nutrient input into the ocean's surface layer and their export as organic matter indicates the CO_2 uptake efficiency of the organic carbon pump (DeVries et al., 2012). This is high in the tropics where the ratio between import and export as regenerated nutrients is close to one. At higher latitudes the transformation of regenerated into preformed nutrients lowers the nutrient import to export ratio and therewith the CO_2 uptake efficiency of the organic carbon pump.

The ballast effect is another process that affects the CO_2 uptake of the organic carbon pump because it increases the water depth at which exported organic matter is respired (e.g. Haake and Ittekkot, 1990; Ittekkot, 1993; Kwon et al., 2009). If organic matter is respired within the euphotic zone, the released CO_2 can immediately return into the atmosphere. If it is respired in the deep sea, regenerated CO_2 and nutrients are injected into the ocean's long-term overturning circulation, where they can be stored for up to 1,500 years (De La Rocha and Passow, 2014; Heinze et al., 1991). Accordingly, the ballast effect strengthens the CO_2 uptake of the organic carbon pump by extending the mean residence time of regenerated nutrients and CO_2 (CO_2 sequestration time) in the ocean (DeVries et al., 2012).

The ballast effect reduces respiration in the water column and increases organic carbon fluxes into the deep mainly due to two processes: minerals, which cause the ballast effect, can (i) adsorb and/or integrate organic molecules onto and into their structure (Armstrong et al., 2002) and (ii) increase the sinking speed of particles in which organic matter is exported from the euphotic zone (Haake and Ittekkot, 1990; Hamm, 2002; Ramaswamy et al., 1991). The former protects organic matter against remineralization and the latter reduces the duration of respiration in the water column. Carbonates, biogenic opal and lithogenic matter are the main ballast minerals. Marine plankton produces carbonates and biogenic opal, whereas lithogenic matter is formed during the weathering of rocks on land. Its input as dust and by rivers into the ocean is thus a steering mechanism linking the CO_2 uptake of the organic carbon pump directly to processes on land (Ittekkot and Haake, 1990).

Results obtained from sediment trap experiments in the northern Indian Ocean have indicated that the Asian monsoon and its impact on the nutrient supply into the euphotic zone controls organic carbon fluxes into the deep Arabian Sea and the Bay of Bengal (Haake et al., 1993; Ittekkot et al., 1991; Nair et al., 1989; Rixen et al., 1996; Rixen et al., 2009). Additionally, eolian dust inputs and discharges from rivers are assumed to influence the ballast effect in these two basins (Ittekkot, 1993; Ittekkot and Haake, 1990). Due to a stronger ballast effect an enhanced share of the organic matter exported from the euphotic zone reached the deep sea in the river-dominated Bay of Bengal (Rao et al., 1994). Export of organic carbon from the euphotic

defines the export production, which is often assumed to correspond to the organic carbon flux at a water-depth of 100 m. In the following we will adopt this definition of the term 'export production' and use the term 'organic carbon flux' for the organic carbon fluxes measured by sediment traps in the deep sea.

In contrast to results obtained from the early sediment trap experiments a Multiple Linear Regression Analysis (MLR) using a global compilation of sediment trap data, including data from the Indian Ocean, showed that primary production hardly affects organic carbon fluxes and that carbonate is the main ballast mineral controlling the organic carbon export into the deep sea in the world's ocean (Klaas and Archer, 2002). This result was supported by Francois et al. (2002) and it was assumed that the contribution of lithogenic matter was too low to significantly contribute to the ballast effect, except in near-shore regions such as the Bay of Bengal. Based on an expanded global compilation of sediment trap data, a geographically weighted analysis identified carbonate and lithogenic matter as the main ballast minerals in the Arabian Sea and the Bay of Bengals (Wilson et al., 2012), whereas an MLR applied to data from the Indian Ocean emphasised the role of biogenic opal as the main ballast mineral (Ragueneau et al., 2006). Therewith, all mineral components (lithogenic matter, carbonate and biogenic opal) were suggested to act as the 'main ballast material' in the Indian Ocean and the role of primary production as the main driver of organic carbon fluxes was called into question. In order to study the influence of primary production and the impact of individual ballast minerals on organic carbon fluxes in the Indian Ocean in more detail we compiled our sediment trap results (Fig. 1, Tab. 1), compared them with satellite data, and applied the MLR to our newly assembled data set. Furthermore, densities of ballast minerals were compiled from the literature and used jointly with measured fluxes and satellite-derived export production rates to calculate sinking speeds and organic carbon fluxes. This mechanistic approach is used to validate conclusions obtained by comparing time-series observations and using statistical methods as well as to quantify impacts of individual ballast minerals on sinking speed and organic carbon fluxes.

2. Study Area

The Asian monsoon strongly influences the northern Indian Ocean with its two semi-enclosed basins: the Arabian Sea and the Bay of Bengal. Sea-level pressure differences between the Asian landmass and the Indian Ocean drive the monsoon (Ramage, 1987, 1971). Following the pressure gradient and deflected by the Coriolis force, wind blows from the NE over the Arabian Sea and the Bay of Bengal in winter between December and February (Currie et al., 1973). In summer (June - September), the situation reverses. The heating of the Asian landmass leads to the formation of a strong atmospheric low which attracts and enforces the SE trade winds to cross the equator in the western Indian Ocean. They form a strong low-level jet (Findlater Jet) blowing from the SW over the Arabian Sea (Fig. 2a,b, Findlater, 1969; Findlater, 1977).

In the Arabian Sea, the positive wind stress curl west of the axis of the Findlater Jet causes upwelling, which is strongest along the coast of the Arabian Peninsula (Bauer et al., 1991; Luther and O'Brien, 1990; Ryther and Menzel, 1965; Sastry and D'Souza, 1972). Weaker upwelling systems also occur NE off Sri Lanka and along the SW coast of India (Sharma, 1978; Shetye et al., 1990; Wiggert et al., 2006), whose signals are carried by the Southwest Monsoon Current into the

southern Bay of Bengal (Unger et al., 2003). Due to the northward movements of the SE trade wind systems and the associated reversal of the South Java Current an upwelling system emerges off South Java and Bali almost simultaneously with the development of the Findlater Jet in the Arabian Sea during the boreal summer (Susanto et al., 2001). Off Java and Bali this is actually the winter season but in order to avoid confusion we refer the term 'summer' and 'winter' to the boreal summer and winter, only.

The monsoon rains feed one of the world's largest river systems (Ganges-Brahmaputra-Meghna), which originates in the Himalayas and has its maximum discharge into the Bay of Bengal in summer (Ludwig et al., 1996; Milliman and Meade, 1983; Milliman et al., 1984; Subramanian et al., 1985). Unlike the Indian subcontinent, Indonesia has no major rivers because it comprises relatively small islands. Nevertheless, model studies suggest that the small Indonesian rivers contribute ~11% ($4.26 * 10^{12}$ m^3yr^{-1}) to the global freshwater discharge into the ocean (Syvitski et al., 2005). Due to the high freshwater water inputs, low salinity surface waters (salinity < 33) fringe the continental shelves and margins in the eastern Indian Ocean north of the equator and the high salinity waters (salinity > 35) reflect the negative freshwater balance in the Arabian Sea (Fig. 2c, d).

Inputs of suspended sediments from the Ganges-Brahmaputra-Meghna (1060 Mt yr^{-1}) and Indonesian rivers (1630 Mt yr^{-1}) represent 80% and 20% of the suspended sediment inputs into the Indian and the world's ocean (Milliman and Farnsworth, 2011; Syvitski et al., 2005). Sediment discharge from the Indus into the Arabian Sea only amounts to about 10 Mt yr^{-1} (Milliman and Farnsworth, 2011) and is largely trapped at the Indian continental shelf and margin due to the prevailing current regime (Ramaswamy et al., 1991). In the western part of the Arabian Sea, where the formation of High Salinity Arabian Sea Water (Rochford, 1966; Tchernia, 1980; Tegen and Fung, 1995) shows negligible freshwater inputs (Fig. 2 c,d), eolian dust inputs are the main sources of lithogenic matter (Clemens et al., 1991; Sirocko et al., 1993; Tegen and Fung, 1995).

3. Methods

3.1 Sediment Trap Data

Our sediment trap experiment started in 1986 and was expanded into the Bay of Bengal one year later in 1987. The fieldwork ended around 1998. It was reinitiated in 2007 and 2008, although this could not be followed up due to piracy, which became an issue in the region at that time. The sediment trap sites in the northern and central Bay of Bengal were shifted slightly southward in some years, whereby the stations NBBT and CBBT were spilt into northern (NBBT-N, CBBT-N) and southern sites (NBBT-S, CBBT-S, Fig. 1, Tab. 1). The sediment trap moorings equipped with Mark 6 and 7 time-series sediment traps were deployed for periods of six months to one year with sampling intervals of mostly around 21 days. Haake et al. (1993) and Rixen et al. (1996) describe the sample processing and the analysis of bulk components (organic carbon, carbonate, biogenic opal and lithogenic matter) in detail. Organic carbon fluxes (POC) multiplied by 1.8 results in organic matter fluxes (OM). The lithogenic matter fluxes represent the difference between total flux and fluxes of OM, carbonate and biogenic opal. Fluxes were used to calculate monthly (Fig. 3), seasonal (Tab. 2), annual (Tab. 3) and long-

term annual means (Tab. 3, 4). The considered seasons were summer (June - September), winter (January - April) and transition periods (May and October to December). Annual means were calculated only when particle fluxes were measured for more than 150 days year^{-1}. Since at NEAST our record covers only one season, we calculated a seasonal mean (Tab. 2) but no annual mean.

3.2 Satellite Data

Monthly mean wind speeds and salinity data were derived from the Scatterometer Climatology of Ocean Winds (Risien and Chelton, 2008) and the Soil Moisture and Ocean Salinity (SMOS) satellite mission, respectively (Fig. 2a-d). The SMOS data covering the period between 2010 and 2012 were downloaded from ftp://ftp.icdc.zmaw.de/smos_sss/. Monthly mean satellite-derived sea surface temperatures (SST, Smith et al., 2008) were obtained from ftp://ftp.emc.ncep.noaa.gov/cmb/sst/oimonth_v2/ASCII_UPDATE. Primary production rates (PP, Fig. 2 e,f) derived from the Vertically Generalized Production Model (VGPM, Behrenfeld and Falkowski, 1997) were downloaded from http://www.science.oregonstate.edu/ocean.productivity and averaged as the SST data at around 1 degree around the trap location.

Equations 1 - 3 introduced by Eppley and Peterson (1979), Law et al. (2000) and Henson et al. (2011) were used to convert primary into export production (POC_{Export}).

$$E: POC_{Export} = \begin{matrix} 0.0025 \cdot PP^2 \rightarrow PP < 200 \\ 0.5 \cdot PP \rightarrow PP > 200 \end{matrix} \quad (1)$$

$$L: POC_{Export} = (-0.02 \cdot SST + 0.63) \cdot PP \quad (2)$$

$$H: POC_{Export} = 0.23 \cdot exp^{(-0.08 \cdot SST)} \cdot PP \quad (3)$$

Eppley and Peterson (1979) suggested two different equations for PP < and > 200 g m^{-2} year^{-1}. The monthly mean primary and export production rates converging the period between 2002 and 2015 were used to calculate monthly (Fig. 3), seasonal (Tab. 2) and annual means (Tab. 5).

3.3 Multiple Linear Regression Analysis (MLR)

Similar to other studies (e.g. Klaas and Archer, 2002; Ragueneau et al., 2006; Wilson et al., 2012), a Multiple Linear Regression Analysis was applied to calculate carrying coefficients (f). Here, we used the OLS regression analysis included in the Python module statsmodels:

$$F_{POC}\left[\frac{g}{m^2 \cdot year}\right] = (f_{Lith.} \cdot F_{Lith.}) + (f_{Opal} \cdot F_{Opal}) + (f_{Carb} \cdot F_{Carb.}) \quad (4)$$

(F) represents fluxes of respective bulk components lithogenic matter (Lith.), biogenic opal (Opal) and carbonate (Carb.). In

order to estimate the relative importance of individual ballast minerals (RIB) for the POC flux (F_{POC}), their contribution to the predicted POC flux was calculated.

$$RIB_i[\%] = \frac{100}{F_{POC}} \cdot (f_i \cdot F_i) \quad (5)$$

(i) indicates the different ballast minerals.

3.4 Sinking Speed

In addition to statistical methods, the influence of the individual ballast minerals can also be derived from a more mechanistic approach by quantifying their contribution to the density of the solids (ρ_{solids}):

$$\rho_{solids} = \frac{(Lith\% \cdot D_{lith}) + (OM\% \cdot D_{OM}) + (Opal\% \cdot D_{Opal}) + (Carb.\% \cdot D_{Carb.})}{100} \quad (6)$$

Lith%, OM (=POC*1.8)%, Opal% and Carb% are the percentage of the respective ballast minerals in the sinking particles collected in the sediment traps and (D) represents their density (Tab. 6).

Densities of the bulk component show a wide range and fall below those of their crystalline analogues (Fig. 4). For example, the density of proteins varies between 1.22 to 1.47 g cm^{-3}, whereas the density of organic matter in phytoplankton comprising > 80% of amino acids varies between 1.03 and 1.1 g cm^{-3} (Lee et al., 2004; Logan and Hunt, 1987; Miklasz and Denny, 2010; Quillin and Matthews, 2000). With 0.7 – 0.84 g cm^{-3}, the density of transparent exopolymers (TEP) – which play an essential role for the formation of marine snow – is even below that of seawater (Azetsu-Scott et al., 2004). Other carbohydrates such as cellulose reveal a density of 1.5 g cm^{-3}. The density of calcite – the most common calcium carbonate mineral in the pelagic ocean – is 2.71 g cm^{-3} (Mottana et al., 1978). In turn, coccolithophores and foraminifera tests reveal densities of only 1.55 g cm^{-3} (page 71, Winter and Siesser, 1994) and up to 1.7 g cm^{-3} (Schiebel et al., 2007; Schiebel and Hemleben, 2000). In contrast to opal – which is a hydrous silicon oxide and reveals densities of 1.9 to 2.5 g cm^{-3} – the density of diatom frustules (biogenic opal) varies between 1.46 and 2.0 g cm^{-3} (Csögör et al., 1999; DeMaster, 2003).

The density of lithogenic matter depends on its mineral composition. Clay minerals change their density by adsorbing water, which is most pronounced within the group of smectite. Their density decreases from 2.72 to 1.4 g cm^{-3} during hydration (Osipov, 2012), whereas hydration hardly affects the density of illite, which decreases from 2.75 to 2.72 g cm^{-3}. At our trap sites, illite and quartz dominate lithogenic matter (Ramaswamy et al., 1991; Ramaswamy et al., 1997). Since the density of quartz is 2.65 g cm^{-3}, we used a density of 2.70 ±0.05g cm^{-3} for lithogenic matter. In order to calculate the densities of the solids and sinking speeds of particles, we used a density of 0.9 ±0.2, 1.73 ±0.27, and 1.63 ±0.08 for organic matter, biogenic opal and carbonate, respectively (Tab. 6).

The density of solids is the term describing the effect of mineral particles on the sinking speed of particles in Stoke's law.

Stoke's law derived from the Navier-Stoke equation is a commonly-used parameterisation for calculating the sinking velocity (U) of particles (e.g., Engel et al., 2009; Lal and Lerman, 1975; McCave, 1975; Miklasz and Denny, 2010):

$$U = \frac{(2 \cdot g \cdot \Delta\rho \cdot radius^2)}{9\eta} \quad (7)$$

(g) is the gravitational acceleration and (radius) defines the radius of the sinking particle. (η) is the viscosity and (Δ ρ) represents the excess density of particles over water or – expressed in other words – the difference between the density of the particle ($\rho_{particle}$) and seawater ($\rho_{seawater}$).

$$\Delta\rho = \rho_{particle} - \rho_{seawater} \quad (8)$$

The density of a sinking particle results from its pore water content and the density of the solids:

$$\rho_{particle} = (porosity \cdot \rho_{water}) + (1 - porosity) \cdot \rho_{solids} \quad (9)$$

Sinking speed (U) can be used to estimate the organic carbon flux (POC) at trap depth (z) according to Equation 10 introduced by Banse (1990):

$$POC(z) = POC_{Export} \cdot e^{\left[\frac{-\lambda \cdot (z - depth\ of\ the\ euphotic\ zone)}{sinking\ speed}\right]} \quad (10)$$

(λ) is the POC-specific respiration rate and (POC_{Export}) is the export production. We applied Eqs. 1 - 3 to the satellite-derived primary production rates to calculated export production. (λ) was assumed to vary in a relatively narrow range (0.106 ± 0.028 day^{-1} (Iversen and Ploug, 2010; Ploug and Grossart, 2000), whereas more recent studies suggest that λ decreases with decreasing temperatures (Iversen and Ploug, 2013; Marsay et al., 2015). Direct field observations are scarce (Laufkötter et al., 2017) but *in-situ* incubation experiments carried out at a water depth of < 500 m indicate respiration rates of 0.4 ± 0.1 and 0.01± 0.02 day^{-1} in the subtropical North Atlantic Ocean and the Southern Ocean, respectively (McDonnell et al., 2015). We selected a λ of 0.106 day^{-1}, which is well within this range.

The viscosity of the fluid (η) and the density of sea water (ρ_{water}) were calculated as a function of sea water temperature and salinity by using the Python routines gsw (Gibbs SeaWater) and iapws (International Association for the Properties of Water and Steam*)* (IOC et al., 2010; Wagner and Pruß, 2002). Seawater temperature and salinity were selected from the World Ocean Atlas 2013 (Locarnini et al., 2013; Zweng et al., 2013) for each trap site and averaged between water-depth of 100 and 1500 m (Tab. 5). At our sediment trap sites, the porosity of particles and the radius are unknown. Based on results

derived from other studies, we assume a porosity of 0.917 (Logan and Hunt, 1987).

The equivalent spherical diameters (ESD) of sinking particles cover a wide size spectrum ranging mostly between 0.01 and < 5 mm (Guidi et al., 2009; Iversen et al., 2010). Particles formed in the rolling tanks often exceed 1 mm, reached ESDs of > 1 cm and resemble in size marine snow collected by scuba divers in the surface water of the ocean revealing ESDs of up to 7.5 cm (Alldredge and Gotschalk, 1988; Engel et al., 2009). An ESD of 0.1 mm is a commonly-considered threshold dividing small and large particles (Durkin et al., 2015; Guidi et al., 2009). We selected an ESD of 0.15 mm to calculate sinking speeds.

4. Results and Discussion

4.1 Reliability of sediment trap results

Sediment traps are the only and thus intensively used tool to measure the seasonal and interannual variability of particle fluxes in the ocean (Turner, 2015), but hydrodynamic, biological and chemical processes bias the accuracy of sediment trap measurements (e.g. Antia, 2005; Buesseler et al., 2007). Since current velocities decrease with depth and zooplankton migration is restricted to water depth < 900 m particle fluxes measured at water depth > 1500 m are generally considered as reliable (Bianchi et al., 2013; Honjo et al., 2008). Nevertheless, there are indications that also deep moored traps can undertrap organic matter fluxes by 60% (Buesseler et al., 2007; Buesseler et al., 1992; Scholten et al., 2005; Usbeck et al., 2003; Yu et al., 2001).

In order to estimate possible error ranges we calculated and compared annual mean organic carbon fluxes (Tab. 3). These data show that at JAM off South Java the annual mean organic carbon flux was in 2003 almost twice as high as in the years 2001 and 2002. In contrast to JAM where our record covers only three years we were able to measure particle fluxes over a period of seven and more years at four sites in the northern Indian Ocean. Two of theses sites were in the Arabian Sea (WAST and EAST) and two were in the Bay of Bengal (NBBT-N and SBBT). Among these sites the annual mean organic carbon fluxes revealed the largest variability at WAST. Here we determined the lowest and highest annual mean organic carbon in 1987 and 1997 with 43.0 g C m^{-2} $year^{-1}$ and 69.2 g C m^{-2} $year^{-1}$ respectively (Tab. 3). This represents an increase of about 61%, which may have been caused by undertrapping in 1987, considering an error range of 60%. However, the mean interannual variability was only 16.6 % implying that on the long-term run the reproducibility of the organic carbon fluxes measured by our deep moored traps was much better than the possible error range of 60% and thus the error of the calculated monthly, seasonal, and annual means used in the following discussion is much lower.

4.2 Seasonality and Java in Comparison to the Western Arabian Sea

Previous results obtained from our sediment trap experiments showed a pronounced seasonality with enhanced fluxes during summer and winter, respectively in the Arabian Sea and at JAM off South Java whereas in the Bay of Bengal seasonality was less pronounced (Fig. 3 a,c). The monsoon was assumed to cause the seasonality through its impact on the physical

nutrient supply mechanisms, such as upwelling, vertical mixing, and river discharges in the Bay of Bengal (e.g. Ittekkot et al., 1991; Rixen et al., 2009). Riverine nutrient discharges are assumed to increase organic carbon fluxes within river plumes near the coast but after the consumption of nutrients within the river plume nutrient-depleted freshwater forms a buoyant low salinity surface layer in the open Bay of Bengal (Kumar et al., 1996). This increases stratification in the surface ocean and reduces nutrient inputs during mixed-layer deepening in summer and winter, which in turn weakened the seasonality of organic carbon fluxes at our trap sites in the Bay of Bengal.

Monthly mean satellite-derived primary production rates, which we selected for the trap sites and sediment trap data show a similar seasonality (Fig. 3 b,d). This supports our previous results and the well-known concept of export production, which is driven by inputs of nutrients from the aphotic zone and external reservoirs (the atmosphere and the land) into the euphotic zone (Dugdale and Goering, 1967; Eppley and Peterson, 1979). However, a closer look at the data obtained at JAM and WAST shows that in summer organic carbon fluxes are higher at JAM than at WAST, whereas primary production is lower at JAM than at WAST. Furthermore, low primary production at JAM corresponds with enhanced organic carbon fluxes in winter, which indicates that primary production is not the decisive factor for organic carbon fluxes at JAM.

.

4.3 The Java Mooring (JAM)

At JAM sediment trap data overlap temporally with satellite observation of primary production so that these records can directly be linked to each other (Fig. 3). This comparison shows that enhanced primary production at JAM corresponds to high organic carbon fluxes during the upwelling season in summer 2002, but enhanced fluxes during the rainy season in winter 2002/2003 were not caused by high primary production rates (Fig. 5). This decoupling between satellite-derived primary production and organic carbon fluxes may be caused by a dense cloud cover shading the Indonesian seas from space observations and biasing satellite observations especially in winter (Hendiarti et al., 2004). Additionally, enhanced inputs of resuspended sediments from the shelf could explain the co-occurrence of high organic carbon fluxes and low primary production in winter. However, our data did not indicate a significant input of resuspended sediments. Mg/Ca as well as stable oxygen isotopic ratios of foraminifera shells collected by the trap were used to reconstruct sea water temperatures (Mohtadi et al., 2009). The reconstructed seawater temperatures correlated well with satellite-derived sea surface temperatures, suggesting that inputs of resuspended foraminifera shells biasing sea surface temperature reconstructions could be ignored. Since furthermore organic carbon-to-nitrogen ratios and stable carbon isotopic ratios of organic matter were in the range of marine plankton, impacts of resuspended sediments and terrestrial organic matter were assumed to be negligible at JAM (Rixen et al., 2006).

The ballast effect is another process to decouple primary production and organic carbon flux, especially when river discharges enhance lithogenic matter supply during the rainy season in winter. At JAM the mean lithogenic matter content in winter (68.09%) exceeds that in summer (60.48%, Tab. 2) and suggests that a stronger ballast effect increased the fraction of primary production, which was exported into the deep sea in winter. Considering that JAM has the highest annual mean

lithogenic matter content (61.1%) of our trap sites in the Indian Ocean, a strong lithogenic matter ballast effect is also our explanation for the difference between JAM and WAST.

4.4 Primary Production and Organic Carbon Fluxes

In an attempt to further disentangle impacts of primary production and the ballast effect on the organic carbon flux, seasonal means (Tab. 2) were used to calculate transfer efficiency (T_{eff}) of organic carbon. This defines the ratio between organic carbon fluxes measured by sediment traps and export production and expresses the fraction of export production which reaches the deep sea (Francois et al., 2002). To calculate T_{eff} we converted primary production into export production by using Eqs. 1 to 3. The resulting calculated export production differed between the three equations used: The lowest and highest export production rates were obtained by using Eq. 3 (8 – 49 mg m^{-2} day^{-1}) and Eq. 1 (178 - 639 mg m^{-2} day^{-1}), respectively. Export production is difficult to quantify in the field and constitutes a highly uncertain element in the marine carbon cycle. The wide range of estimates of global mean export production (1.8 - 27.5 10^{15} g C yr^{-1}) reflects this (del Giorgio and Duarte, 2002; Honjo et al., 2008; Lutz et al., 2007). Since we cannot resolve this issue and have no data to validate the calculated export production we used results obtained from all three equation to compute export production rates and T_{eff} (Fig. 6).

Francois et al. (2002) calculated T_{eff} by using Eq. 2 and a global compilation of sediment trap data, which contained also data from the Arabian Sea and the Bay of Bengal. Their results indicated that 9.6 ±4.9% and 16±2.4% of the exported organic carbon arrives at the sediment traps in the Arabian Sea and the Bay of Bengal. Using Eq. 2 like Francois et al. (2002), our annual mean data suggest that 16.5 ±5% and 46.5±5% of the exported organic matter reach the traps, respectively. Different SST values used to calculate export production mainly causes this deviation because Eq. 2 is extremely sensitive to temperature changes. SSTs, which we obtained form Smith et al. (2008) were approximately 0.6° higher than those used by Francois et al. (2002). However, even with these different SST values the resulting shifts in T_{eff} by using Eq. 2 are small in comparison to those caused by using all three equations used to calculate $T_{eff.}$ This indicates that on average 6±3% (Eq.1), 35±19%, (Eq. 2), or 56±22% (Eq.3) of the export production reaches the sediment traps.

It is interesting that independent of which equation is used calculated export production correlates with T_{eff}, whereas T_{eff} increases with decreasing export production (Fig. 6). Francois et al. (2002) obtained a similar result and explained it with a high f-ratio (=export/primary production), which characterizes highly productive diatom blooms. A high f-ratio implies a low recycling efficiency of organic matter in the euphotic zone and thus a reduced transfer of organic matter to higher trophic levels. The low recycling efficiency favours the export of more labile organic matter in marine snow and the reduced transfer of organic matter to higher trophic levels lowers the formation of fast-sinking zooplankton faecal pellets. Consequences include an enhanced export of labile organic matter in slower-sinking marine snow, which in turn favours respiration and lowers T_{eff}.

If we divide our data into two groups, characterized by a lithogenic matter content of < 25% and > 25%, the group with a lithogenic matter content > 25% in general has a higher T_{eff} at similar export production rates (Fig. 6). This suggest that also

the lithogenic content influnces T_{eff} and increase it, if lithogenic matter content exceeds 25%. This is the case in samples collected at our sites in the river-dominated northern and central Bay of Bengal and at JAM. In winter T_{eff} at JAM exceeds even 100% if Eq. 3 is used to calculate export production. This is unrealistic as it means that organic carbon fluxes measured by the trap exceed export production, but it points towards the strong lithogenic matter ballast effect at JAM in winter.

4.5 Carbonate versus Lithogenic Ballast

Since MLR is an often-used approach to study the relative importance of the different ballast minerals we applied it to our data set to further investigate the role of individual ballast minerals on organic carbon fluxes at our trap locations in the Indian Ocean. For this investigation we included data obtained form six sediment traps, which were deployed at a water depth of > 2220 m in the western Arabian Sea off Oman during the US JGOFS program in 1994/95 at sites MS2-5 (Fig. 1, Honjo et al., 1999). Applied to annual means, the MLR shows that the highest carrying coefficients are associated with biogenic opal followed by those of carbonate (Tab. 7). This matches results obtained by Ragueneau et al. (2006) and disagrees with those obtained from the geographically weighted analyses, which identified carbonate and lithogenic matter as the main ballast minerals in the Arabian Sea and the Bay of Bengals (Wilson et al., 2012).

In order to investigate regional differences within the Indian Ocean, we also applied the MLR to the data obtained by analysing the bulk composition of sinking particles collected in the individual sampling cups at each sediment trap site (Tab. 7). On average, this revealed that the highest carrying coefficient in association with lithogenic matter. Weighted by multiplying the carrying coefficients with the associated flux (RIB) indicates that on average lithogenic matter ballast contributes 43 ±19% to the predicted organic carbon fluxes (Tab. 8). This varies regionally and identifies carbonate as main ballast mineral at WAST. In contrast to our previous results, carbonate is also suggested as the main ballast mineral at JAM, which is surprising considering the low carbonate and the high content of lithogenic matter in samples from these sites (Tab. 4, 5).

To gain more clarity we correlated organic carbon fluxes with the content of the individual ballast materials. Lithogenic matter content correlates with organic carbon fluxes measured in the Indian Ocean when its content exceeds 25% (Fig. 7a). If lithogenic matter content is < 25% organic carbon fluxes correlate best with carbonate fluxes and shows no obvious link to the lithogenic matter content (Fig. 7b). This implies that lithogenic matter is the dominant ballast material at our trap sites in the river-influenced regions whereas carbonate is the main ballast mineral at the other locations in the open Indian Ocean. Alternatively, the correlation between carbonate and organic carbon fluxes could also be a consequence of a joint production. This is obvious in blooms dominated by coccolithophorids, as well as in those dominated by non-calcifying phytoplankton when e.g. calcifying grazers such as pelagic foraminifera prevail. In the western Arabian Sea this is indicated by peak fluxes of pelagic foraminifera, which coincide with upwelling-driven diatom blooms (Haake et al., 1993). Foraminifera test are incorporated in sinking particles but sink also on their own with sinking speeds of several hundred-metres day^{-1} (Schiebel, 2002; Schiebel and Hemleben, 2005; Schmidt et al., 2014). However, in contrast to carbonate lithogenic matter mostly consists of clay minerals (Ramaswamy et al., 1991), which are too small to sink on their own

(Honjo, 1976; McCave, 1975; Rex and Goldberg, 1958). It owes its transport into the deep sea mainly to its incorporation into organic particles suggesting that the correlation between lithogenic matter content and organic carbon fluxes reflects the lithogenic matter ballast effect.

4.6 Sinking Speeds and organic carbon fluxes

Eqs. 6 – 10 were used to calculate sinking speeds and organic carbon fluxes by using flux rates and satellite-derived export production rates to further demonstrate that primary production and lithogenic matter control the variability of organic carbon fluxes at our trap locations in the open Indian Ocean and river-influenced regions, respectively. Furthermore, this mechanistic approach allows us to quantify the impact of the individual ballast minerals on sinking speeds and organic carbon fluxes.

To calculate the density of the solids (ρ_{solids}) and the sinking speed of particles, the densities of bulk components were compiled from the literature (Tab. 6). Due to the high density of lithogenic matter its content mainly controls sinking speeds as indicated by the correlation between lithogenic matter content and sinking speed (Fig. 8a). The mean calculated sinking speed is 224±33 m day^{-1} and agrees with sinking speeds of > 214 m day^{-1}, which were derived from the temporal delay of about 14 days between the onset of upwelling and the associated increase of organic fluxes at water depth of about 3000 m in the Arabian Sea (Rixen et al., 1996). Furthermore, it falls within the range of sinking speeds (230 ±72 m day^{-1}) obtained from the US JGOFS sediment trap experiment in the Arabian Sea (Berelson, 2001) showing that our calculated sinking speeds and the chosen parameter values to calculate it, are in an acceptable range (Tab. 6).

In a second step the calculated sinking speeds and satellite-derived export production were used to calculate organic carbon fluxes (Eq. 10). Independent of which equation we used to compute export production, the calculated organic carbon fluxes correlate with the measured ones (Fig. 8 b,c), but organic carbon fluxes obtained by using Eq.1 and 2 were higher and those obtained by using Eq. 3 were lower than the measured fluxes. The varying calculated organic carbon fluxes are a consequence of the different export production rates, which results by applying Eqs. 1 to 3 to the satellite-derived primary production as mentioned before. The best agreement between measured and calculated fluxes could be achieved by using Eq. 3 and changing the constant in Eq.3 from 0.23 to 0.40 (Fig. 8c).

To further entangle the role of primary production and the ballast effect on organic carbon fluxes we computed organic carbon fluxes by using constant sinking speed of 206.5 m day^{-1} and the modified Eq. 3. The mean deviation between organic carbon fluxes calculate with sinking speed of 206.5 and those derived from calculated sinking speeds are close to zero at sampling sites characterized by a lithogenic matter content < 25%. The r-value obtained form this regression analysis is 0.919 (n=12). The correlation between measured and calculated organic carbon fluxes for which we used a constant sinking speed suggests that export production rather than the ballast effect controls the spatial variability of organic carbon fluxes and explains the correlation between carbonate and organic carbon fluxes as shown in Figure 7b.

At the sites in the open Indian Ocean carbonate reveals the highest contribution (> 45%) to the density of ballast minerals and could thus be considered as main ballast mineral (Fig. 9). Since primary production increases organic and carbonate fluxes and lowers T_{eff} (Fig. 6) it is assumed that the role of the carbonate ballast as indicated by the contribution of carbonate to the density of solids is an overestimate due to carbonate shells which sink on their own in highly productive systems such as the western Arabian Sea. At sites in river-influenced regions of the Indian Ocean lithogenic matter reveals a contribution to the density of ballast material, which exceeds those at other minerals (Fig. 9). Organic carbon fluxes computed with a constant sinking speed of 206.6 m day^{-1} are on average 20% and at JAM even 35% lower as the one derived from the calculated sinking speeds and lithogenic matter sinks incorporated into organic particles. Accordingly, it is assumed that lithogenic matter ballast strongly affected organic carbon fluxes at sediment trap locations in the river-influenced regions of the Indian Ocean. Considering that primary production obtained at our locations in this region varied between 0.31 (CBBT-S) and 0.53 g m^{-2} day^{-1} (JAM) and ranged between 0.31 (SBBT) and 1.15 g m^{-2} day^{-1} (MS2, Tab. 5) at sites in open Indian Ocean a lower variability of primary production seems to favour the determined impact of lithogenic matter on the organic carbon in the river-influenced regions of the Indian Ocean, additionally (Fig. 7a).

In order to quantify the impact of the lithogenic matter ballast effect on the organic carbon fluxes we conducted a numerical experiment. We assumed a lithogenic matter flux of zero and recalculated the contribution of the other ballast minerals to the total flux minus the lithogenic matter. This reduced the mean sinking speed from 224 ± 33 to 147 ±5 m day^{-1} (Fig. 8a) and the resulting mean calculated organic carbon fluxes by 41% and 51% at sites in open Indian Ocean and the river-influenced regions of the Indian Ocean. Consequently, lithogenic matter ballast seems to be an important factor increasing organic fluxes at all sites in the Indian Ocean while primary production controls the spatial variability of organic carbon fluxes measured at the trap sites in the open Indian Ocean, due to its high variability. This differs at the studied locations in the river-influenced regions of the Indian Ocean and at JAM the high lithogenic matter content increased the calculated organic carbon flux even by 62%, which could explain the compared to WAST high measured organic carbon flux. Such an increase of organic carbon flux due to lithogenic matter inputs from land emphasizes the role of land use changes on the residence time of regenerated CO_2 and the associated CO_2 uptake efficiency of the organic carbon pump. Considering the Neolithic revolution and the estimated of an up to twenty-fold increase of erosion due to deforestation and the expansion of agriculture (Neil, 2014), humans must have increased the ballast effect and the CO_2 uptake of the organic carbon already over thousands of years..

5. Conclusion

The evaluation of our data in conjunction with satellite-derived observations shows that primary production mainly controls the spatial variability of organic carbon fluxes at the study sites in the open Indian Ocean. Since primary production increased carbonate and organic carbon fluxes and lowered T_{eff} it is assumed that in highly productive systems the role of carbonate as ballast mineral as indicated by its contribution to the density of solids, is an overestimate. An enhanced export

of carbonate shells sinking on their own could cause this. In the river-influenced northern and central Bay of Bengal and off South Java lithogenic matter ballast was the main ballast material and its content strongly influenced the spatial variability of organic carbon fluxes favoured a weakly pronounced variability of primary production in these regions.

Calculate sinking speeds and organic carbon fluxes indicate that lithogenic matter could increase the mean sinking speeds by 34% and the mean calculated organic carbon flux by 41% and 51% at sites in the open Indian Ocean and river-influenced regions of the Indian Ocean, respectively. Accordingly, lithogenic matter seems to increase organic carbon fluxes at all studied sites in the Indian Ocean whereas primary production controls the spatial variability of organic carbon fluxes measured at the trap sites in the open Indian Ocean, due to high variability of primary production in this region. This differs at sites in the river-influenced areas of the Indian Ocean and an enhanced lithogenic matter content increased the calculated organic carbon fluxes even by up to 62%. This agrees to the high measured organic carbon fluxes in the compared to the western Arabian Sea low-productive South Java Sea.

Acknowledgments

First of all, we would like to thank all of the scientists, technicians, officers and their crews of the numerous research vessels used during our studies in the Indian Ocean. We would specifically like to express our gratitude to the Federal German Ministry for Education, Science, Research and Technology (BMBF, Bonn ref. no. 03F0463A), the Council of Scientific and Industrial Research (CSIR, New Delhi), the Ministry of Earth Sciences (MOES, New Delhi), and the Agency for the Assessment and Application of Technology (BPPT), Jakarta, Indonesia for financial support. P. Wessels and W.H.F Smith are acknowledged for providing the generic mapping tools (GMT).

References

Alldredge, A. L. and Gotschalk, C.: In situ setting behavior of marine snow, Limnology and Oceanography, 33, 339-351, 1988.

Antia, A. N.: Solubilization of particles in sediment traps: revising the stoichiometry of mixed layer export, Biogeosciences, 2, 189-204, 2005.

Archer, D. E., Eshel, G., Winguth, A., Broecker, W., Pierrehumbert, R., Tobis, M., and Jacob, R.: Atmospheric pCO_2 sensitivity to the biological pump in the ocean, Global Biogeochemical Cycles, 14, 1219-1230, 2000.

Armstrong, R. A., Lee, C., Hedges, J. I., Honjo, S., and Wakeham, S.: A new, mechanistic model for organic carbon fluxes in the ocean: based on the quantitative association of POC with ballast minerals, Deep Sea Research, 49, 219 - 236, 2002.

Avnimelech, Y., Troeger, B. W., and Reed, L. W.: Mutual Flocculation of Algae and Clay: Evidence and Implications, Science, 216, 63-65, 1982.

Azetsu-Scott, Kumiko, and Passow, U.: Ascending marine particles: Significance of transparent exopolymer particles (TEP) in the upper ocean, Limnology Oceanography, 49, 741 - 748, 2004.

Banse, K.: New views on the degradation and disposition of organic particles as collected by sediment traps in the open sea, Deep Sea Research, 37, 1177-1195, 1990.

Bauer, S., Hitchcock, G. L., and Olson, D. B.: Influence of monsoonally-forced Ekman dynamics upon surface layer depth and plankton biomass distribution in the Arabian Sea, Deep Sea Research, 38, 531-553, 1991.

Behrenfeld, M. J. and Falkowski, P. G.: Photosynthetic rates derived from satellite-based chlorophyll concentration, Limnology and Oceanography, 42, 1-20, 1997.

Berelson, W. M.: Particle settling rates increase with depth in the ocean, Deep Sea Research Part II: Topical Studies in Oceanography, 49, 237-251, 2001.

Bianchi, D., Galbraith, E. D., Carozza, D. A., Mislan, K. A. S., and Stock, C. A.: Intensification of open-ocean oxygen depletion by vertically migrating animals, Nature Geosci, 6, 545-548, 2013.

Bopp, L., Resplandy, L., Orr, J. C., Doney, S. C., Dunne, J. P., Gehlen, M., Halloran, P., Heinze, C., Ilyina, T., Séférian, R., Tjiputra, J., and Vichi, M.: Multiple stressors of ocean ecosystems in the 21st century: projections with CMIP5 models, Biogeosciences, 10, 6225-6245, 2013.

Broecker, W. S., Takahashi, T., and Takahashi, T.: Sources and Flow Patterns of Deep-Ocean Waters as Deduced From Potential Temperature, Salinity, and Initial Phosphate Concentration, Journal of Geophysical Research, 90, 6925-6939, 1985.

Buesseler, K. O., Antia, A. N., Chen, M., Fowler, S. W., Gardner, W. D., Gustafsson, O., Harada, K., Michaels, A. F., Rutgers van der Loeff, M., Sarin, M., Steinberg, D. K., and Trull, T.: An assessment of the use of sediment traps for estimating upper ocean particle fluxes, Journal of Marine Research,, 65, 345 - 416, 2007.

Buesseler, K. O., Bacon, M. P., Kirk Cochran, J., and Livingston, H. D.: Carbon and nitrogen export during the JGOFS North Atlantic Bloom experiment estimated from 234Th: 238U disequilibria, Deep Sea Research Part A. Oceanographic Research Papers, 39, 1115-1137, 1992.

Cartapanis, O., Bianchi, D., Jaccard, S. L., and Galbraith, E. D.: Global pulses of organic carbon burial in deep-sea sediments during glacial maxima, Nat Commun, 7, 2016.

Clemens, S., Prell, W., Murray, D., Shimmield, G., and Weedon, G.: Forcing mechanisms of the Indian Ocean monsoon, Nature, 353, 720-725, 1991.

Csögör, Z., Melgar, D., Schmidt, K., and Posten, C.: Production and particle characterization of the frustules of Cyclotella cryptica in comparison with siliceous earth, Journal of Biotechnology, 70, 71-75, 1999.

Currie, R. I., Fisher, A. E., and Hargreaves, P. M.: Arabian Sea Upwelling. In: Biology of the Indian Ocean, 1973.

De La Rocha, C. L. and Passow, U.: 8.4 - The Biological Pump. In: Treatise on Geochemistry (Second Edition), Turekian, H. D. H. K. (Ed.), Elsevier, Oxford, 2014.

del Giorgio, P. A. and Duarte, C. M.: Respiration in the open ocean, Nature, 420, 379-384, 2002.

DeMaster, D. J.: 7.04 - The Diagenesis of Biogenic Silica: Chemical Transformations Occurring in the Water Column, Seabed, and Crust A2 - Turekian, Heinrich D. HollandKarl K. In: Treatise on Geochemistry, Pergamon, Oxford, 2003.

DeVries, T. and Deutsch, C.: Large-scale variations in the stoichiometry of marine organic matter respiration, Nature Geosci, 7, 890-894, 2014.

DeVries, T., Primeau, F., and Deutsch, C.: The sequestration efficiency of the biological pump, Geophysical Research Letters, 39, L13601, 2012.

Duce, R. A., LaRoche, J., Altieri, K., Arrigo, K. R., Baker, A. R., Capone, D. G., Cornell, S., Dentener, F., Galloway, J., Ganeshram, R. S., Geider, R. J., Jickells, T., Kuypers, M. M., Langlois, R., Liss, P. S., Liu, S. M., Middelburg, J. J., Moore, C. M., Nickovic, S., Oschlies, A., Pedersen, T., Prospero, J., Schlitzer, R., Seitzinger, S., Sorensen, L. L., Uematsu, M., Ulloa, O., Voss, M., Ward, B., and Zamora, L.: Impacts of Atmospheric Anthropogenic Nitrogen on the Open Ocean, Science, 320, 893-897, 2008.

Dugdale, R. C. and Goering, J. J.: Uptake of new and regenerated forms of nitrogen in primary productivity., Limnology and Oceanography, 12, 196-206, 1967.

Durkin, C. A., Estapa, M. L., and Buesseler, K. O.: Observations of carbon export by small sinking particles in the upper mesopelagic, Marine Chemistry, 175, 72-81, 2015.

Duteil, O., Koeve, W., Oschlies, A., Aumont, O., Bianchi, D., Bopp, L., Galbraith, E., Matear, R., Moore, J. K., Sarmiento, J. L., and Segschneider, J.: Preformed and regenerated phosphate in ocean general circulation models: can right total concentrations be wrong?, Biogeosciences, 9, 1797-1807, 2012.

Engel, A., Szlosek, J., Abramson, L., Liu, Z., and Lee, C.: Investigating the effect of ballasting by CaCO3 in Emiliania huxleyi: I. Formation, settling velocities and physical properties of aggregates, Deep Sea Research Part II: Topical Studies in Oceanography, 56, 1396-1407, 2009.

Eppley, R. W. and Peterson, B. J.: Particulate organic matter flux and planktonic new production in the deep ocean, Nature, 282, 677-680, 1979.

Falkowski, P. G., Barber, R. T., and Smetacek, V.: Biogeochemical Controls and Feedbacks on Ocean Primary Production, Science, 281, 200-206, 1998.

Findlater, J.: A major low-level air current near the Indian Ocean during the northern summer, Quart. J. R. Met. Soc., 95, 362-380, 1969.

Findlater, J.: A Numerical Index to Monitor the Afro-Asian Monsoon During the Northern Summers, Meteorological Magazine, 106, 170-180, 1977.

France-Lanord, C. and Derry, L. A.: Organic carbon burial forcing of the carbon cycle from Himalayan erosion, Nature, 390, 65-67, 1997.

Francois, R., Honjo, S., Krishfield, R., and Manganini, S.: Factors controlling the flux of organic carbon to the bathypelagic zone of the ocean, Global Biogeochemical Cycles, 16, 34-31 - 34-20, 2002.

Galy, V., France-Lanord, C., Beyssac, O., Faure, P., Kudrass, H., and Palhol, F.: Efficient organic carbon burial in the Bengal fan sustained by the Himalayan erosional system, Nature, 450, 407-410, 2007.

Garrison, D. L., Gowing, M. M., and Hughes, M. P.: Nano- and microplankton in the northern Arabian Sea during the Southwest Monsoon, August-September 1995 A US-JGOFS study, Deep Sea Research Part II: Topical Studies in Oceanography, 45, 2269-2299, 1998.

Garrison, D. L., Gowing, M. M., Hughes, M. P., Campbell, L., Caron, D. A., Dennett, M. R., Shalapyonok, A., Olson, R. J., Landry, M. R., and Brown, S. L.: Microbial food web structure in the Arabian Sea: a US JGOFS study, Deep Sea Research II, 47, 1387-1422, 2000.

Guidi, L., Stemmann, L., Jackson, G. A., Ibanez, F., Claustre, H., Legendre, L., Picheral, M., and Gorskya, G.: Effects of phytoplankton community on production, size, and export of large aggregates: A world-ocean analysis, Limnology and Oceanography, 54, 1951-1963, 2009.

Gust, G., Byrne, R. H., Bernstein, R. E., Betzer, P. R., and Bowles, W.: Particle fluxes and moving fluids: experience from synchronous trap collections in the Sargasso Sea, Deep Sea Research, 39, 1071-1083, 1992.

Gust, G., Michaels, A. F., Johnson, R., Deuser, W. G., and Bowles, W.: Mooring line motions and sediment trap hydromechanics: in situ intercomparison of three common deployment designs, Deep Sea Research I, 41, 831-857, 1994.

Haake, B. and Ittekkot, V.: Die Wind-getriebene "biologische Pumpe" und der Kohlenstoffentzug im Ozean, Naturwissenschaften, 77, 75-79, 1990.

Haake, B., Ittekkot, V., Rixen, T., Ramaswamy, V., Nair, R. R., and Curry, W. B.: Seasonality and interannual variability of particle fluxes to the deep Arabian Sea, Deep Sea Research I, 40, 1323-1344, 1993.

Hamm, C. E.: Interactive aggregation and sedimentation of diatoms and clay-sized lithogenic material, Limnology and Oceanography, 47, 1790-1795, 2002.

Heinze, C., Maier-Reimer, E., and Winn, K.: Glacial pCO_2 Reduction by the World Ocean: Experiments with the Hamburg Carbon Cycle Model, Paleoceanography, 6, 395-430, 1991.

Hendiarti, N., Siegel, H., and Ohde, T.: Investigation of different coastal processes in Indonesian water using SeaWiFS data., Deep Sea Research, 51, 85-97, 2004.

Henson, S. A., Sanders, R., Madsen, E., Morris, P. J., Le Moigne, F., and Quartly, G. D.: A reduced estimate of the strength of the ocean's biological carbon pump, Geophysical Research Letters, 38, L04606, 2011.

Honjo, S.: Coccoliths: Production, Transportation and Sedimentation, Marine Micropaleontology, 1, 65-79, 1976.

Honjo, S.: Seasonality and Interaction of Biogenic and Lithogenic Particulate Flux at the Panama Basin, Science, 218, 883-884, 1982.

Honjo, S., Dymond, J., Prell, W., and Ittekkot, V.: Monsoon-controlled export fluxes to the interior of the Arabian Sea, Deep Sea Research II, 46, 1859-1902, 1999.

Honjo, S., Manganini, S. J., Krishfield, R. A., and Francois, R.: Particulate organic carbon fluxes to the ocean interior and factors controlling the biological pump: A synthesis of global sediment trap programs since 1983, Progress in Oceanography, 76, 217-285, 2008.

IOC, SCOR, and IAPSO: The international thermodynamic equation of seawater - 2010: Calculation and use of thermodynamic properties., Intergovernmental Oceanographic Commission UNESCO Manuals and Guides, 196 pp., 2010.

Ito, T. and Follows, M. J.: Preformed phosphate, soft tissue pump and atmospheric CO_2, Journal of Marine Research, 63, 813 - 839, 2005.

Ittekkot, V.: The abiotically driven biological pump in the ocean and short-term fluctuations in atmospheric CO_2 contents, Global and Planetary Change, 8, 17-25, 1993.

Ittekkot, V. and Haake, B.: The Terrestrial Link in the Removal of Organic Carbon in the Sea. In: Factes of Modern Biogeochemistry, Ittekkot, V., Kempe, S., Michaelis, W., and Spitzy, A. (Eds.), Springer Verlag, Berlin, Heidelberg, New York, 1990.

Ittekkot, V., Nair, R. R., Honjo, S., Ramaswamy, V., Bartsch, M., Manganini, S., and Desai, B. N.: Enhanced particle fluxes in Bay of Bengal induced by injection of fresh water, Nature, 351, 385-387, 1991.

Iversen, M. H., Nowald, N., Ploug, H., Jackson, G. A., and Fischer, G.: High resolution profiles of vertical particulate organic matter export off Cape Blanc, Mauritania: Degradation processes and ballasting effects, Deep Sea Research Part I: Oceanographic Research Papers, 57, 771-784, 2010.

Iversen, M. H. and Ploug, H.: Ballast minerals and the sinking carbon flux in the ocean: carbon-specific respiration rates and sinking velocity of marine snow aggregates, Biogeosciences, 7, 2613-2624, 2010.

Iversen, M. H. and Ploug, H.: Temperature effects on carbon-specific respiration rate and sinking velocity of diatom aggregates – potential implications for deep ocean export processes, Biogeosciences, 10, 4073-4085, 2013.

Iversen, M. H. and Robert, M. L.: Ballasting effects of smectite on aggregate formation and export from a natural plankton community, Marine Chemistry, 175, 18-27, 2015.

Jahnke, R. A.: The global ocean flux of particulate organic carbon: Areal distribution and magnitude, Global Biogeochemical Cycles, 10, 71-88, 1996.

Keeling, C. D. and Whorf, T. P.: Atmospheric CO_2 concentrations (ppmv) derived from in situ air samples collected at Mauna Loa Observatory, Hawaii, Scrips Institution of Oceanography, University of California La Jolla, California USA 92093 - 04444, 2005. 2005.

Keil, R. G. and Hedges, J. I.: Sorption of organic matter to mineral surfaces and the preservation of organic matter in coastal marine sediments, Chemical Geology, 107, 385-388, 1993.

Klaas, C. and Archer, D. E.: Association of sinking organic matter with various types of mineral ballast in the deep sea: Implications for the rain ratio., Global Biogeochemical Cycles, 16, doi:10.1029/2001GB001765, 2002.

Knox, F. and McElroy, M. B.: Changes in atmospheric CO2: Influence of the marine biota at high latitude, Journal of Geophysical Research: Atmospheres, 89, 4629-4637, 1984.

Koning, E., Brummer, G.-J., Van Raaphorst, W., Van Bennekom, J., Helder, W., and Van Iperen, J.: Settling, dissolution and burial of biogenic silica in the sediments off Somalia (northwestern Indian Ocean), Deep Sea Research Part II: Topical Studies in Oceanography, 44, 1341-1360, 1997.

Kranck, K.: Flocculation of Suspended Sediment in the Sea, Nature, 246, 348-350, 1973.

Kumar, D., M., Naqvi, S. W. A., George, M. D., and Jayakumar, A.: A sink for atmospheric carbon dioxide in the northeastern Indian Ocean, Journal of Geophysical Research, 101, 18,121 - 118,125, 1996.

Kwon, E. Y., Primeau, F., and Sarmiento, J. L.: The impact of remineralization depth on the air-sea carbon balance, Nature Geosci, 2, 630-635, 2009.

Lal, D. and Lerman, A.: Size spectra of biogenic particles in ocean water and sediments, Journal of Geophysical Research, 80, 423-430, 1975.

Laufkötter, C., John, J. G., Stock, C. A., and Dunne, J. P.: Temperature and oxygen dependence of the remineralization of organic matter, Global Biogeochemical Cycles, 31, 1038-1050, 2017.

Laws, E. A., Falkowski, P. G., Smith, W. O., Ducklow, H., and McCarthy, J. J.: Temperature effects on export production in the open ocean, Global Biogeochemical Cycles, 14, 1231-1246, 2000.

Le Moigne, F. A. C., Pabortsava, K., Marcinko, C. L. J., Martin, P., and Sanders, R. J.: Where is mineral ballast important for surface export of particulate organic carbon in the ocean?, Geophysical Research Letters, 41, 8460-8468, 2014.

Lee, C., Hedges, J. I., Wakeham, S. G., and Zhu, N.: Effectiveness of various treatments in retarding microbial activity in sediment trap material and their effects on the collection of swimmers, Limnology and Oceanography, 37, 117-130, 1992.

Lee, C., Murray, D. W., Barber, R. T., Buesseler, K. O., Dymond, J., Hedges, J. I., Honjo, S., Manganini, S. J., and Marra, J.: Particulate organic carbon fluxes: compilation of results from the 1995 US JGOFS Arabian Sea Process Study, Deep Sea Research II, 45, 2489-2501, 1998.

Lee, C., Wakeham, S. G., and Arnosti, C.: Particulate organic matter in the sea: the composition conundrum, Ambio, 33, 565-575, 2004.

Locarnini, R. A., Mishonov, A. V., Antonov, J. I., Boyer, T. P., Garcia, H. E., Baranova, O. K., Zweng, M. M., Paver, C. R., Reagan, J. R., Johnson, D. R., Hamilton, M., and Seidov, D.: World Ocean Atlas 2013, National Oceanographic Data Center(NODC), 2013.

Logan, B. E. and Hunt, J. R.: Advantages to microbes of growth in permeable aggregates in marine systems1, Limnology and Oceanography, 32, 1034-1048, 1987.

Ludwig, W., Probst, J.-L., and Kempe, S.: Predicting the oceanic input of organic carbon by continental erosion, Global Biogeochemical Cycles, 10, 23-41, 1996.

Luther, M. E. and O'Brien, J. J.: Variability in Upwelling Fields in the Northwestern Indian Ocean - 1. Model Experiments for the Past 18,000 Years, Paleoceanography, 5, 433-445, 1990.

Lutz, M. J., Caldeira, K., Dunbar, R. B., and Behrenfeld, M. J.: Seasonal rhythms of net primary production and particulate organic carbon flux to depth describe the efficiency of biological pump in the global ocean, Journal of Geophysical Research: Oceans, 112, C10011, 2007.

Marsay, C. M., Sanders, R. J., Henson, S. A., Pabortsava, K., Achterberg, E. P., and Lampitt, R. S.: Attenuation of sinking particulate organic carbon flux through the mesopelagic ocean, Proceedings of the National Academy of Sciences of the United States of America, 112, 1089-1094, 2015.

McCave, I. N.: Size Spectra and aggregation of suspended particles in the deep ocean, Deep Sea Research, 31, 329-352, 1984.

McCave, I. N.: Vertical flux of particles in the ocean, Deep Sea Research, 22, 491-502, 1975.
McDonnell, A. M. P., Boyd, P. W., and Buesseler, K. O.: Effects of sinking velocities and microbial respiration rates on the attenuation of particulate carbon fluxes through the mesopelagic zone, Global Biogeochemical Cycles, 29, 175-193, 2015.
Miklasz, K. A. and Denny, M. W.: Diatom sinkings speeds: Improved predictions and insight from a modified Stokes' law, Limnology and Oceanography, 55, 2513-2525, 2010.
Milliman, J. D. and Farnsworth, K. L.: River discharge to the coastal ocean, Cambridge University Press, Cambridge, 2011.
Milliman, J. D. and Meade, R. H.: World-Wide Delivery of River Sediment to the Oceans, The Journal of Geology, 91, 1-21, 1983.
Milliman, J. D., Quraishee, G. S., and Beg, M. A. A.: Sediment discharge from the Indus River to the ocean: past, present and future. In: Marine Geology and Oceanography of Arabian Sea and Coastal Pakistan, Haq, B. U. and Milliman, J. D. (Eds.), Van Nostrand Reinhold Company Scientific and Academic Editions, New York, Cincinnati, Stroudsburg, Toronto, London, Melbourne, 1984.
Mohtadi, M., Steinke, S., Groeneveld, J., Fink, H., G., Rixen, T., Hebbeln, D., Donner, B., and Herunadi, B.: Low-latitude control on seasonal and interannual changes in planktonic foraminiferal flux and shell geochemistry off south Java: A sediment trap study, Paleoceanography, 24, PA1201, 2009.
Mottana, A., Crespi, R., and Liborio, G.: Simon & Schuster's guide to rocks & minerals, Simon and Schuster, New York, 1978.
Nair, R. R., Ittekkot, V., Manganini, S. J., Ramaswamy, V., Haake, B., Degens, E. T., Desai, B. N., and Honjo, S.: Increased particle flux to the deep ocean related to monsoons, Nature, 338, 749-751, 1989.
Neil, R.: The Holocene: An Environmental History, Wiley-Blackwell, Hoboken, New Jersey USA, 2014.
Nielsen, E. S.: Measurement of the Production of Organic Matter in the Sea by means of Carbon-14, Nature, 167, 684-685, 1951.
Osipov, V. I.: Density of clay minerals, Soil Mechanics and Foundation Engineering, 48, 231-240, 2012.
Pabortsava, K., Lampitt, R. S., Benson, J., Crowe, C., McLachlan, R., Le Moigne, F. A. C., Mark Moore, C., Pebody, C., Provost, P., Rees, A. P., Tilstone, G. H., and Woodward, E. M. S.: Carbon sequestration in the deep Atlantic enhanced by Saharan dust, Nature Geosci, 10, 189-194, 2017.
Palamenghi, L., Schwenk, T., Spiess, V., and Kudrass, H. R.: Seismostratigraphic analysis with centennial to decadal time resolution of the sediment sink in the Ganges–Brahmaputra subaqueous delta, Continental Shelf Research, 31, 712-730, 2011.
Passow, U. and Carlson, C. A.: The biological pump in a high CO2 world, Marine Ecology Progress Series, 470, 249-271, 2012.

Ploug, H. and Grossart, H.-P.: Bacterial growth and grazing on diatom aggregates: Respiratory carbon turnover as a function of aggregate size and sinking velocity, Limnology and Oceanography, 45, 1467-1475, 2000.

Quillin, M. L. and Matthews, B. W.: Accurate calculation of the density of proteins, Acta Crystallographica Section D, 56, 791-794, 2000.

Ragueneau, O., Schultes, S., Bidle, K., Claquin, P., and Moriceau, B.: Si and C interactions in the world ocean: Importance of ecological processes and implications for the role of diatoms in the biological pump, Global Biogeochemical Cycles, 20, GB4S02, 2006.

Ramage, C. S.: Monsoon Climates. In: The Encyclopedia of Climatology, Oliver, J. E. and Fairbridge, R. W. (Eds.), Van Nostrand Reinhold Company, New York, 1987.

Ramage, C. S.: Monsoon Meteorology, Academic Press, New York, London, 1971.

Ramaswamy, V., Nair, R. R., Manganini, S., Haake, B., and Ittekkot, V.: Lithogenic fluxes to the deep Arabian Sea measured by sediment traps, Deep Sea Research, 38, 169-184, 1991.

Ramaswamy, V., Vijay Kumar, B., Parthiban, G., Ittekkot, V., and Nair, R. R.: Lithogenic fluxes in the Bay of Bengal measured by sediment traps, Deep Sea Research Part I: Oceanographic Research Papers, 44, 793-810, 1997.

Ramesh Kumar, M. R. and Prasad, T. G.: Annual and interannual variation of precipitation over the tropical Indian Ocean, Journal of Geophysical Research, 102, 18,519-518,527, 1997.

Ramesh Kumar, M. R. and Schlüssel, P.: Air-Sea Interaction over the Indian Ocean During the Two Contrasting Monsoon Years 1987 and 1988 Studied with Satellite Data, Theor. Appl. Climatol., 60, 219-231, 1998.

Rao, C. K., Naqvi, S. W. A., Kumar, M. D., Varaprasad, S. J. D., Jayakumar, D. A., George, M. D., and Singbal, S. Y. S.: Hydrochemistry of the Bay of Bengal: possible reasons for a different water-column cycling of carbon and nitrogen from the Arabian Sea, Marine Chemistry, 47, 279-290, 1994.

Rex, R. W. and Goldberg, E. D.: Quartz Contents of Pelagic Sediments of the Pacific Ocean1, Tellus, 10, 153-159, 1958.

Riebesell, U., Schulz, K. G., Bellerby, R. G. J., Botros, M., Fritsche, P., Meyerhofer, M., Neill, C., Nondal, G., Oschlies, A., Wohlers, J., and Zollner, E.: Enhanced biological carbon consumption in a high CO_2 ocean, Nature, 450, 545-548, 2007.

Risien, C. M. and Chelton, D. B.: A Global Climatology of Surface Wind and Wind Stress Fields from Eight Years of QuikSCAT Scatterometer Data, Journal of Physical Oceanography, 38, 2379-2413, 2008.

Rixen, T., Guptha, M. V. S., and Ittekkot, V.: Sedimentation. In: Report of the Indian Ocean Synthesis Group on the Arabian Sea Process Study, Watts, L., Burkill, P. H., and Smith, S. (Eds.), JGOFS International Project Office, Bergen, 2002.

Rixen, T., Haake, B., Ittekkot, V., Guptha, M. V. S., Nair, R. R., and Schlüssel, P.: Coupling between SW monsoon-related surface and deep ocean processes as discerned from continuous particle flux meausurements and correlated satellite data, Journal of Geophysical Research, 101, 28,569-528,582, 1996.

Rixen, T., Ittekkot, V., Herundi, B., Wetzel, P., Maier-Reimer, E., and Gaye-Haake, B.: ENSO-driven carbon see saw in the Indo-Pacific, Journal of Geophysical Research Letters, 33, doi:10.1029/2005GL024965, 2006.

Rixen, T., Ramaswamy, V., Gaye, B., Herunadi, B., Maier-Reimer, E., Bange, H. W., and Ittekkot, V.: Monsoonal and ENSO Impacts on Export Fluxes and the Biological Pump in the Indian Ocean In: Indian Ocean Biogeochemical Processes and Ecological Variability, Hood, R. R., Wiggert, J. D., Naqvi, S. W. A., Smith , S., and Brink , K. (Eds.), 185, AGU, Washington, 2009.

Rochford, D. J.: Source regions of oxygen maxima in intermediate depths of the Arabian Sea, Marine and Freshwater Research, 17, 1-30, 1966.

Romero, O. E., Rixen, T., and Herunadi, B.: Effects of hydrographic and climatic forcing on diatom production and export in the tropical southeastern Indian Ocean, Marine Ecology Progress Series, 384, 69-82, 2009.

Ryther, J. H. and Menzel, D. W.: On the production composition and distribution of organic matter in the Western Arabian Sea, Deep Sea Research, 12, 199-209, 1965.

Sabine, C. L. and Tanhua, T.: Estimation of Anthropogenic CO_2 Inventories in the Ocean, Annual Review of Marine Science, 2, 175-198, 2009.

Sarmiento, J. L. and Gruber, N.: Ocean Biogeochemical Dynamics, Princeton University Press, Princeton New Jersey, 2006.

Sarmiento, J. L. and Toggweiler, J. R.: A new model for the role of the oceans in determining atmospheric pCO_2, Nature, 308, 621-624, 1984.

Sastry, J. S. and D'Souza, R. S.: Upwelling & Upward Mixing in the Arabian Sea, Indian Journal of Marine Sciences, 1, 17-27, 1972.

Schiebel, R.: Planktic foraminiferal sedimentation and the marine calcite budget, Global Biogeochemical Cycles, 16, 13-11 - 13-21, 2002.

Schiebel, R., Barker, S., Lendt, R., Thomas, H., and Bollmann, J.: Planktic foraminiferal dissolution in the twilight zone, Deep Sea Research Part II: Topical Studies in Oceanography, 54, 676-686, 2007.

Schiebel, R. and Hemleben, C.: Interannual variability of planktic foraminiferal populations and test flux in the eastern North Atlantic Ocean (JGOFS), Deep Sea Research Part II: Topical Studies in Oceanography, 47, 1809-1852, 2000.

Schiebel, R. and Hemleben, C.: Modern planktic foraminifera, Paläontologische Zeitschrift, 79, 135 - 148, 2005.

Schmidt, K., De La Rocha, C. L., Gallinari, M., and Cortese, G.: Not all calcite ballast is created equal: differing effects of foraminiferan and coccolith calcite on the formation and sinking of aggregates, Biogeosciences, 11, 135-145, 2014.

Scholten, J., Fietzke, J., Mangini, A., Stoffers, P., Rixen, T., Gaye-Haake, B., Blanz, T., Ramaswamy, V., Sirocko, F., Schulz, H., and Ittekkot, V.: Radionuclide fluxes in the Arabian Sea: the role of particle composition, Earth and Planetary Science Letters, 230, 319 - 337, 2005.

Schott, F. and McCreary, J. P., Jr.: The monsoon circulation of the Indian Ocean, Progress in Oceanography, 51, 1 - 123, 2001.

Sharma, G. S.: Upwelling Off the Soutwest Coast of India, Indian Journal of Marine Sciences, 7, 209-218, 1978.

Shetye, S. R., Gouveia, A. D., Shenoi, S. S. C., Sundar, D., Michael, G. S., Almeida, A. M., and Santanam, K.: Hydrography and circulation off the west coast of India during the Southwest Monsoon 1987, Journal of Marine Research, 48, 359-378, 1990.

Siegel, D. A., Buesseler, K. O., Doney, S. C., Sailley, S. F., Behrenfeld, M. J., and Boyd, P. W.: Global assessment of ocean carbon export by combining satellite observations and food-web models, Global Biogeochemical Cycles, 28, 181-196, 2014.

Siegenthaler, U. and Wenk, T.: Rapid atmospheric CO_2 variations and ocean circulation, Nature, 308, 624-627, 1984.

Sirocko, F., Sarnthein, M., Erlenkeuser, H., Lange, H., Arnold, M., and Duplessy, J. C.: Century-scale events in monsoonal climate over the past 24,000 years, Nature, 364, 322-324, 1993.

Smith , S., L.: The Arabian Sea of the 1990s: New Biogeochemical Understanding, Progress In Oceanography, 65, 113 - 290, 2005.

Smith, S. L.: The northwestern Indian Ocean during the monsoons of 1979: distribution, abundance, and feeding of zooplankton, Deep Sea Research, 29, 1331-1353, 1982.

Smith, T. M., Reynolds, R. W., Peterson, T. C., and Lawrimore, J.: Improvements to NOAA's historival merged land-ocean surface temperature analysis (1880 - 2006), Journal of Climate, 21, 2283 - 2296, 2008.

Subramanian, V., Richey, J. E., and Abbas, N.: Geochemistry of River Basins of India Part II - Preliminary Studies on the Particulate C and N in the Ganges-Brahmaputra River System, Mitt. Geol.-Paläont. Inst. Univ. Hamburg, 58, 513-518, 1985.

Susanto, R. D., Gordon, A. L., and Zengh, Q.: Upwelling along the coasts of Java and Sumatra and its relation to ENSO, Journal of Marine Research Letters, 28, 1599-1602, 2001.

Syvitski, J. P. M., Vörösmarty, C. J., A.J., K., and Green, P.: Impact of humans on the flux of terrestrial sediment to the global ocean, Science, 308, 376 - 380, 2005.

Tchernia, P.: Descriptive regional oceanography, Oxford Pergamon Press, Oxford, UK, 1980.

Tegen, I. and Fung, I.: Contribution to the atmospheric mineral aerosol load from land surface modification, Journal of Geophysical Research, 100, 18,707-718,726, 1995.

Turner, J. T.: Zooplankton fecal pellets, marine snow, phytodetritus and the ocean's biological pump, Progress in Oceanography, 130, 205-248, 2015.

Unger, D., Ittekkot, V., Schäfer, P., and Tiemann, J.: Biogeochemistry of particulate organic matter from the Bay of Bengal as discernible from hydrolysable neutral carbohydrates and amino acids, Marine Chemistry, 96, 155-184, 2005.

Unger, D., Ittekkot, V., Schafer, P., Tiemann, J., and Reschke, S.: Seasonality and interannual variability of particle fluxes to the deep Bay of Bengal: influence of riverine input and oceanographic processes, Deep Sea Research Part II: Topical Studies in Oceanography, 50, 897-923, 2003.

Usbeck, R., Schlitzer, R., Fischer, G., and Wefer, G.: Particle fluxes in the ocean: comparison of sediment trap data with results from inverse modeling, Journal of Marine Systems, 39, 167-183, 2003.

Volk, T. and Hoffert, M. I.: The carbon cycle and atmospheric CO_2, natural variation archean to present. In: The Carbon Cycle and Atmospheric CO_2: Natural Variations Archean to Present, Sundquist, E. T. and Broecker, W. S. (Eds.), AGU, Washington, 1985.

Wagner, W. and Pruß, A.: The IAPWS Formulation 1995 for the Thermodynamic Properties of Ordinary Water Substance for General and Scientific Use, Journal of Physical and Chemical Reference Data, 31, 387-535, 2002.

Westberry, T. K., Williams, P. J. l. B., and Behrenfeld, M. J.: Global net community production and the putative net heterotrophy of the oligotrophic oceans, Global Biogeochemical Cycles, 26, GB4019, 2012.

Wiggert, J. D., Murtugudde, R. G., and Christian, J. R.: Annual ecosystem variability in the tropical Indian Ocean: Results of a coupled bio-physical ocean general circulation model, Deep Sea Research Part II: Topical Studies in Oceanography, 53, 644-676, 2006.

Wilson, J. D., Barker, S., and Ridgwell, A.: Assessment of the spatial variability in particulate organic matter and mineral sinking fluxes in the ocean interior: Implications for the ballast hypothesis, Global Biogeochemical Cycles, 26, GB4011, 2012.

Winter, A. and Siesser, W. G.: Coccolithophores, Cambridge University Press, New York, 1994.

Yu, E.-F., Francois, R., Bacon, M. P., Honjo, S., Fleer, A. P., Manganini, S. J., Rutgers van der Loeff, M. M., and Ittekkot, V.: Trapping efficiency of bottom-tethered sediment traps estimated from the intercepted fluxes of ^{230}Th and ^{231}Pa, Deep Sea Research I, 48, 865-889, 2001.

Zweng, M. M., Reagan, J. R., Antonov, J. I., Locarnini, R. A., Mishonov, A. V., Boyer, T. P., Garcia, H. E., Baranova, O. K., Paver, C. R., Johnson, D. R., Seidov, D., and Biddle, M.: World Ocean Atlas 2013, National Oceanographic Data Center(NODC), 2013.

Captions

Figure 1: Bathymetric chart of the northern Indian Ocean and the adjacent land mass. Data were obtained from http://Ingrid.ldgo. Columbia.edu/SOURCE/WORLDBATH. White circles show the sediment trap sites operated by the joint Indo/German and Indonesian German projects (see Tab. 1). The black circles represent the US JGOFS sediment trap site M2 to M5 (Honjo et al., 1999; Lee et al., 1998).

Figure 2. Monthly mean wind speeds (a, b), derived from the Scatterometer Climatology of Ocean Winds (Risien and Chelton, 2008) indicating the Findlater Jet during the summer (August) in the Arabian Sea. Monthly mean sea surface salinities (c, d) derived from the Soil Moisture and Ocean Salinity (SMOS) satellite mission. Monthly mean primary production rates (Behrenfeld and Falkowski, 1997) covering the periods between 2002 and 2014 (e, f). The black circles show the sediment trap sites (Fig. 1, Tab. 1).

Figure 3: Monthly mean organic carbon fluxes (POC) obtained from our sediment trap experiments in the Arabian Sea (a) and the Bay of Bengal (c) as well as monthly mean primary production rates (Behrenfeld and Falkowski, 1997) selected for the sediment trap sites (b, d). The sediment trap data were normalized to a water depth of 2000 m by using the equation introduced by Rixen et al. (2002).

Figure 4: Densities of bulk components including quartz and illite as representatives of lithogenic matter (red lines, and circle). Black circles and lines indicate the densities of crystalline analogues and of cellulose as an example of a carbohydrate. The data were compiled from the literature and the references are given in the text. The grey area shows the density range of seawater.

Figure 5: Organics carbon fluxes measure at JAM and the primary production rates selected for the JAM site.

Figure 6: T_{eff} versus export production rates derived from equation 1 (a), 2 (b) and 3 (c). The red circle indicate samples associated with lithogenic matter content < 25%.

Figure 7: Organic carbon fluxes (POC) versus lithogenic matter content (a) and carbonate flux (b). The red and black circle indicate trap sites at which the annual mean lithogenic matter content is < and > 25%, respectively.

Figure 8: (a) Annual mean lithogenic matter content at the trap sites in the Indian Ocean versus sinking speeds derived from the density of the solids (Eqs. 6 - 9) including the regression equation and line. The red circle indicates sinking speeds derived from the US JGOFS sediment trap sites in the western Arabian Sea (Berelson, 2001) and the blue circle represents sinking speeds derived from the density of the solids by setting the lithogenic matter flux to zero. (b) Annual mean organic carbon fluxes determined at the sediment trap sites versus organic carbon fluxes calculated by using Eq.10 and sinking speed shown in figure 8 a. The export production was derived from Eq.1 (red circles), 2 (blue circles), and 3 (black circles). The red colour shows the regression equation and line obtained from the correlation between the calculated and measured fluxes whereas the respective export production used to calculate the organic carbon flux was derived from Eq.1. The black line indicates the 1:1 line (c) Calculated versus measured fluxes as in (b) but the modified Eq.3 was used to calculate the required export production. The errors bars indicate the interannual variability of the measured fluxes and the range caused the variability of the sinking speeds used to calculate the organic carbon flux.

Figure 9. Annual mean contribution of lithogenic matter, carbonate, and biogenic opal to the density of the ballast material. Blue and red squares indicate data characterised by a lithogenic matter content < and > 25% , respectively.

Table 1. Number of station, trap ID, station name, position, water-depth, trap depth, seawater temperature and salinity.

No.	Trap ID	Name	Lat.	Lon.	W-Depth	T-Depth
			[°N]	[°N]	[m]	[m]
1	WAST	Western Arabian Sea Trap Station	16.26	60.58	4032	3017
2	CAST	Central Arabian Sea Trap Station	14.51	64.72	3920	2944
3	EAST	Eastern Arabian Sea Trap Station	15.57	68.73	3791	2870
4	NEAST	Northeastern Arabian Sea Trap Station	16.93	67.84	3545	3039
5	SAST	Southern Arabian Sea Trap Station	11.60	66.08	4243	3032
6	EIOT	Equatorial Indian Ocean Trap Station	3.56	77.78	3400	2374
7	NBBT-N	Northern Bay of Bengal Trap Station – North	17.42	89.65	2267	1889
8	NBBT-S	Northern Bay of Bengal Trap Station – South	15.48	89.45	2709	2172
9	CBBT-N	Central Bay of Bengal Trap Station – North	13.14	84.41	3266	2261
10	CBBT-S	Central Bay of Bengal Trap Station – South	11.03	84.43	3462	2527
11	SBBT	Southern Bay of Bengal Trap Station	5.09	87.26	3995	2976
12	JAM	Java Mooring	-8.28	108.02	3250	2456

Table 2. Trap ID, season, seasonal averaged primary production, sea surface temperature, organic carbon flux and lithogenic matter content.

Trap ID	Season	PP [g m^{-2} day^{-1}]	SST [°C]	POC [mg m^{-2} day^{-1}]	Lith. Matter [%]
WAST	summer	1.28	25.60	11.69	14.46
WAST	winter	0.79	26.32	7.50	15.39
WAST	transition	0.49	27.90	6.48	13.04
CAST	summer	1.11	26.76	6.95	16.73
CAST	winter	0.70	26.93	6.41	14.55
CAST	transition	0.42	28.32	5.52	15.85
EAST	summer	0.57	27.56	6.82	21.39
EAST	winter	0.46	27.41	5.28	19.91
EAST	transition	0.30	28.63	5.05	21.97
SAST	summer	0.56	27.78	6.65	14.21
SAST	winter	0.34	27.98	6.46	15.75
SAST	transition	0.30	28.75	3.91	14.87
SBBT	summer	0.39	28.39	7.91	15.04
SBBT	winter	0.27	29.00	5.34	17.48
SBBT	transition	0.29	28.85	5.29	15.27
EIOT	summer	0.38	28.75	4.55	10.13
EIOT	winter	0.27	29.06	3.90	18.50
EIOT	transition	0.34	28.92	4.07	11.65
CBBT-N	summer	0.31	28.98	8.03	38.90
CBBT-N	winter	0.32	27.90	8.00	36.14
CBBT-N	transition	0.29	28.92	7.64	44.89
CBBT-S	summer	0.35	28.95	5.13	24.33
CBBT-S	winter	0.30	28.16	5.15	32.45
CBBT-S	transition	0.30	28.97	6.19	21.99
NBBT-N	summer	0.39	28.82	9.74	41.99
NBBT-N	winter	0.34	27.15	7.05	38.06
NBBT-N	transition	0.29	28.80	6.92	38.98
NBBT-S	summer	0.34	28.73	5.91	32.39
NBBT-S	winter	0.30	27.53	6.03	33.49
NBBT	transition	0.27	28.93	6.17	32.76
JAM	summer	0.86	27.09	14.35	60.48
JAM	winter	0.31	29.08	11.47	68.09
JAM	transition	0.49	28.48	11.75	60.36
NEAST	transition	0.33	28.13	8.80	29.82

Table 3. Annual mean total fluxes measured at the trap sites during the years from 1986 to 2003 in the g C m^{-2} $year^{-1}$ including the mean and the standard deviation as well as the number of years (no) in which particle fluxes were measured for more than 150 days $year^{-1}$.

Trap ID	86	87	88	89	90	91	92	93	94	95	96	97	98	1	2	3	Mean	Std.	No.
	[g C m^{-2} $year^{-1}$]																	[%]	
WAST	45.0	43.0	53.6		66.0	50.6	48.5		52.9	58.6		69.2					54.1	16.6	9
CAST	34.8	34.4	40.7					35.0	40.3		40.0						37.5	8.2	6
EAST	37.4	35.4	34.4	39.0	34.8	37.5		23.3	39.3			34.8					35.1	13.7	9
SAST								43.7									43.7		1
EIOT										35.0	21.3	26.9					27.7	24.7	3
NBBT-N			53.2	50.2					53.4	44.9	47.5	38.9	46.1				47.7	10.7	7
NBBT-S						33.4	34.0										33.7	1.3	2
CBBT-N			43.5	56.7	66.4	60.7		44.8									54.4	18.3	5
CBBT-S							34.8										34.8		1
SBBT			39.9			37.3	35.5	37.2	42.3	47.0	40.5	39.6					39.9	9.0	8
JAM														101.8	122.1	201.2	141.7	37.0	3

Table 4. Trap ID, annual mean bulk fluxes including standard deviation (std) and contents. The standard deviation indicates the interannual variability.

Trap ID	POC	std	Carb.	std	Opal	std	Lith.	std	POC	Carb.	Opal	Lith.
	[g m-2 year-1]								[%]			
WAST	3.1	0.4	29.0	3.5	13.1	3.9	7.9	1.5	5.6	52.3	23.5	14.2
CAST	2.3	0.2	22.4	1.3	4.8	0.4	5.9	0.8	6.1	60.1	12.9	15.9
EAST	2.1	0.3	17.9	2.1	5.4	1.1	7.3	1.1	6.1	52.2	15.8	21.1
SAST	2.3	0.0	27.1	0.0	6.0	0.0	6.5	0.0	5.2	62.0	13.6	15.0
EIOT	1.5	0.3	16.4	3.1	5.2	1.3	3.6	0.9	5.4	58.7	18.7	12.8
NBBT-N	2.9	0.3	13.3	1.9	10.4	0.7	18.8	3.9	6.1	27.9	21.8	39.5
NBBT-S	2.2	0.0	11.0	0.4	7.7	0.4	11.1	0.3	6.5	32.5	22.9	32.9
CBBT-N	2.9	0.3	15.5	1.0	11.7	2.3	21.9	5.9	5.3	28.5	21.6	40.3
CBBT-S	2.0	0.0	13.4	0.0	8.9	0.0	9.0	0.0	5.7	38.4	25.6	25.7
SBBT	2.3	0.3	20.0	1.8	9.8	1.5	6.1	1.4	5.6	50.0	24.6	15.3
JAM	4.8	0.6	15.1	2.5	31.3	15.6	86.6	23.9	3.4	10.7	22.1	61.1

Table 5. Trap ID, annual mean primary production (PP) and sea surface temperature (SST) as well as seawater temperature (Temp) and salinity. Temp and salinity were selected for trap sites from the World Ocean Atlas 2013 and averaged between water-depth of 100 and 1500 m. Density and viscosity were calculate by using Temp and salinity, considering a water-depth of 800 m. Python routines 'gsw' and iapws were used for these calculations. In addition to our trap site also data for the US JGFOS trap site MS2-5 were selected. Figure 1 shows the location of these sites.

Station ID	PP	SST	Temp.	Salinity	Density	Viscosity
	[g m^{-2} day^{-1}]	[°C]	[°C]		[g cm^{-3}]	[kg m^{-1} s^{-1}]
WAST	0.79	26.93	11.48	35.49	1.030511	0.001217
CAST	0.69	27.57	11.22	35.43	1.030517	0.001225
EAST	0.42	28.07	11.11	35.42	1.030529	0.001229
SAST	0.38	28.38	10.63	35.29	1.030525	0.001244
NEAST	0.49	27.81	11.32	35.47	1.030527	0.001222
EIOT	0.33	29.05	9.34	35.01	1.030555	0.001287
NBBT-N	0.33	28.25	9.42	34.96	1.030505	0.001285
NBBT-S	0.30	28.43	9.42	34.96	1.030505	0.001285
CBBT-N	0.31	28.57	9.38	34.96	1.030510	0.001286
CBBT-S	0.31	28.70	9.36	34.98	1.030526	0.001286
SBBT	0.31	28.91	9.33	34.99	1.030542	0.001288
JAM	0.53	28.33	8.25	34.69	1.030496	0.001326
MS2	1.15	26.48	11.53	35.52	1.030523	0.001215
MS3	0.97	26.60	11.56	35.52	1.030518	0.001214
MS4	0.74	27.11	11.35	35.45	1.030509	0.001221
MS5	0.32	28.43	10.32	35.22	1.030529	0.001254

Table 6. Values used to calculate sinking speeds (Eqs.6 - 9). Densities of the bulk components were obtained from the literature.

	Value	Unit
POC-specific respiration rate (λ)	0.120	day^{-1}
Porosity	0.917	
Radius	0.150	mm
Density of the ballast material		
OM	0.90 ±0.20	g cm^{-3}
Opal	0.73 ±0.27	g cm^{-3}
Carb.	1.63 ±0.08	g cm^{-3}
Lith.	2.70 ±0.05	g cm^{-3}

Table 7. Carrying coefficients derived from the MLR applied to data measured at the trap sites (Trap ID) including the mean. 'No.' indicates the number of data used for the analysis. A-Trap shows the carrying coefficients derived by applying the MLR to the annual mean sediment data obtained from our sites (No. = 11) and including the US JGOFS data (No. = 17). CA-Trap shows carrying coefficients obtained from all annual means (our and US JGOFS data) including a constant term to Ep. 4.

Trap ID	$CaCO_3$	Std.	P val.	Opal	Std.	P val.	Lith.	Std.	P val.	r^2	No.
WAST	0.044	0.007	0.000	0.046	0.007	0.000	0.132	0.018	0.000	0.958	142
CAST	0.018	0.007	0.008	0.198	0.032	0.000	0.120	0.026	0.000	0.955	88
EAST	0.033	0.007	0.000	0.124	0.020	0.000	0.108	0.014	0.000	0.970	115
SAST	0.011	0.004	0.034	0.049	0.028	0.111	0.256	0.029	0.000	0.998	13
EIOT	0.031	0.008	0.000	0.035	0.034	0.303	0.227	0.029	0.000	0.963	39
NBBT-N	0.090	0.011	0.000	0.070	0.015	0.000	0.046	0.005	0.000	0.973	88
NBBT-S	-0.022	0.031	0.480	0.139	0.048	0.008	0.126	0.023	0.000	0.964	26
CBBT-N	0.096	0.008	0.000	0.057	0.012	0.000	0.033	0.005	0.000	0.972	78
CBBT-S	0.017	0.019	0.372	0.078	0.025	0.011	0.115	0.028	0.002	0.982	13
SBBT	0.041	0.006	0.000	0.073	0.011	0.000	0.115	0.014	0.000	0.960	99
JAM	0.128	0.026	0.000	0.034	0.013	0.010	0.022	0.005	0.000	0.943	54
Mean	0.044	0.012		0.082	0.022		0.118	0.018			
A-Trap	0.067	0.018	0.006	0.113	0.062	0.105	0.006	0.021	0.761	0.983	11
A-Trap	0.073	0.013	0.000	0.116	0.046	0.024	0.004	0.015	0.789	0.989	17
CA-Trap	0.066	0.018	0.002	0.120	0.048	0.026	0.002	0.016	0.913	0.922	17

Table 8. Contribution of the individual ballast minerals to the predicted POC flux (RIB see Eq. 5)

Trap	$CaCO_3$	Opal	Lith.
WAST	47.0	17.8	35.1
CAST	21.1	46.2	32.7
EAST	31.0	30.9	38.1
SAST	13.4	12.8	73.8
EIOT	37.0	11.8	51.2
NBBT-N	42.8	24.5	32.7
NBBT-S	-11.9	51.6	60.4
CBBT-N	55.2	21.4	23.4
CBBT-S	12.0	34.7	53.2
SBBT	36.0	30.9	33.1
JAM	41.1	19.1	39.7
Mean	29.5	27.4	43.0

5

Figure 1

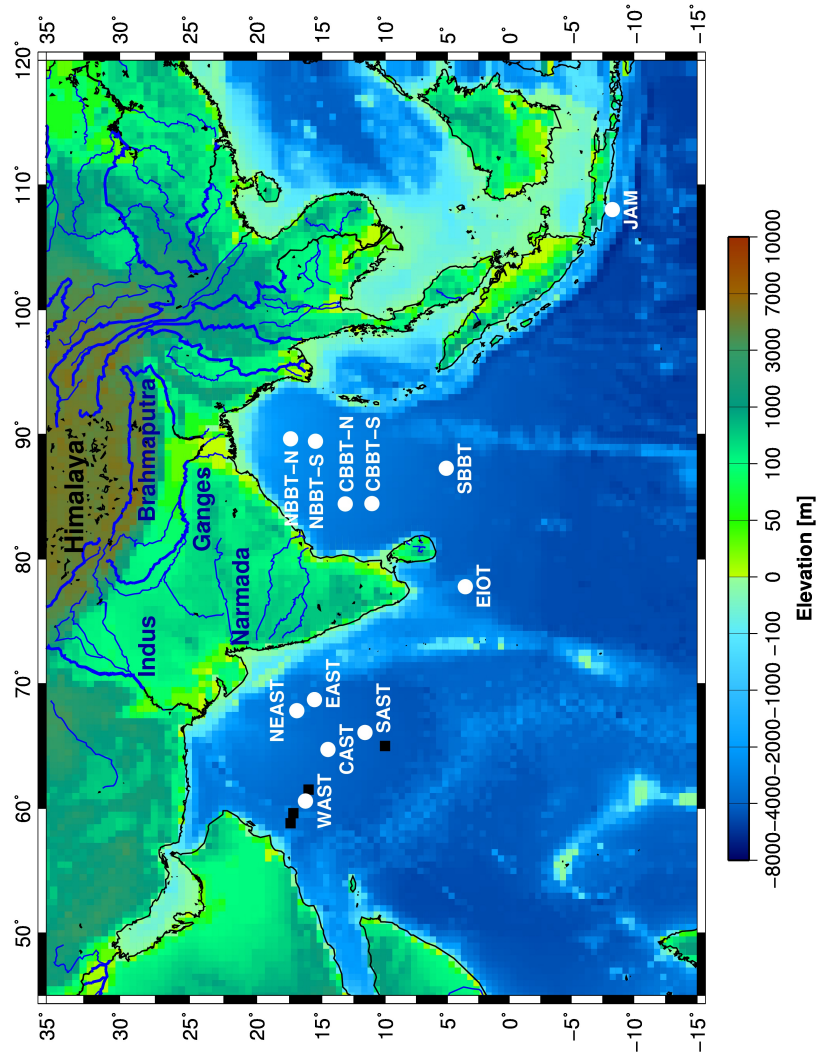
Himalaya
Brahmaputra
Ganges
Narmada
Indus
NBBT–N
NBBT–S
CBBT–N
CBBT–S
SBBT
EIOT
JAM
NEAST
EAST
CAST
SAST
WAST
Elevation [m]
−8000 −4000 −2000 −1000 −100 0 50 100 1000 3000 7000 10000

Figure 2

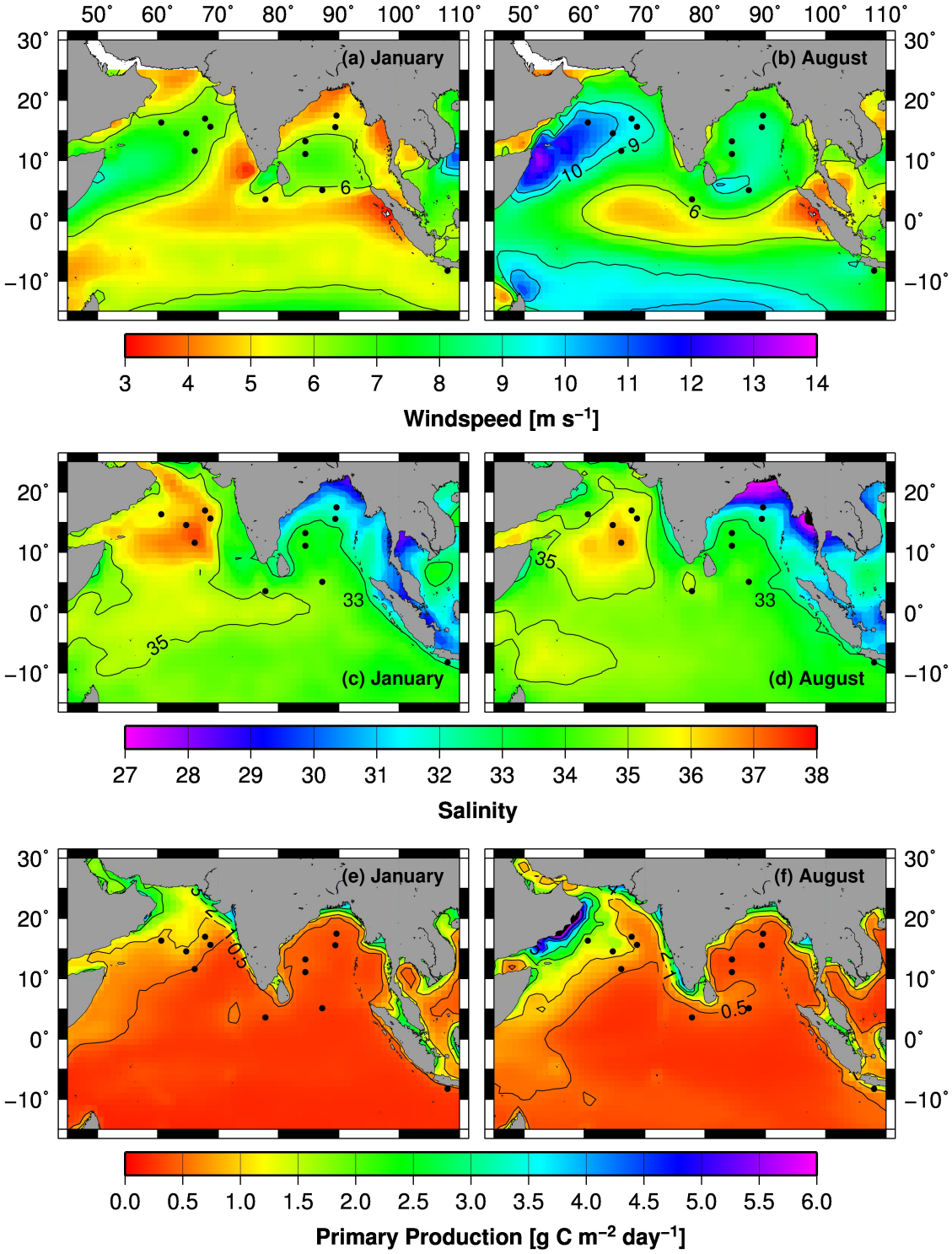
50° 60° 70° 80° 90° 100° 110°
30° 20° 10° 0° −10°
(a) January
(b) August
6
9
10
6
3 4 5 6 7 8 9 10 11 12 13 14
Windspeed [m s−1]
20° 10° 0° −10°
33
35
(c) January
(d) August
27 28 29 30 31 32 33 34 35 36 37 38
Salinity
(e) January
(f) August
0.5
1
0.5
0.0 0.5 1.0 1.5 2.0 2.5 3.0 3.5 4.0 4.5 5.0 5.5 6.0
Primary Production [g C m−2 day−1]

Figure 3

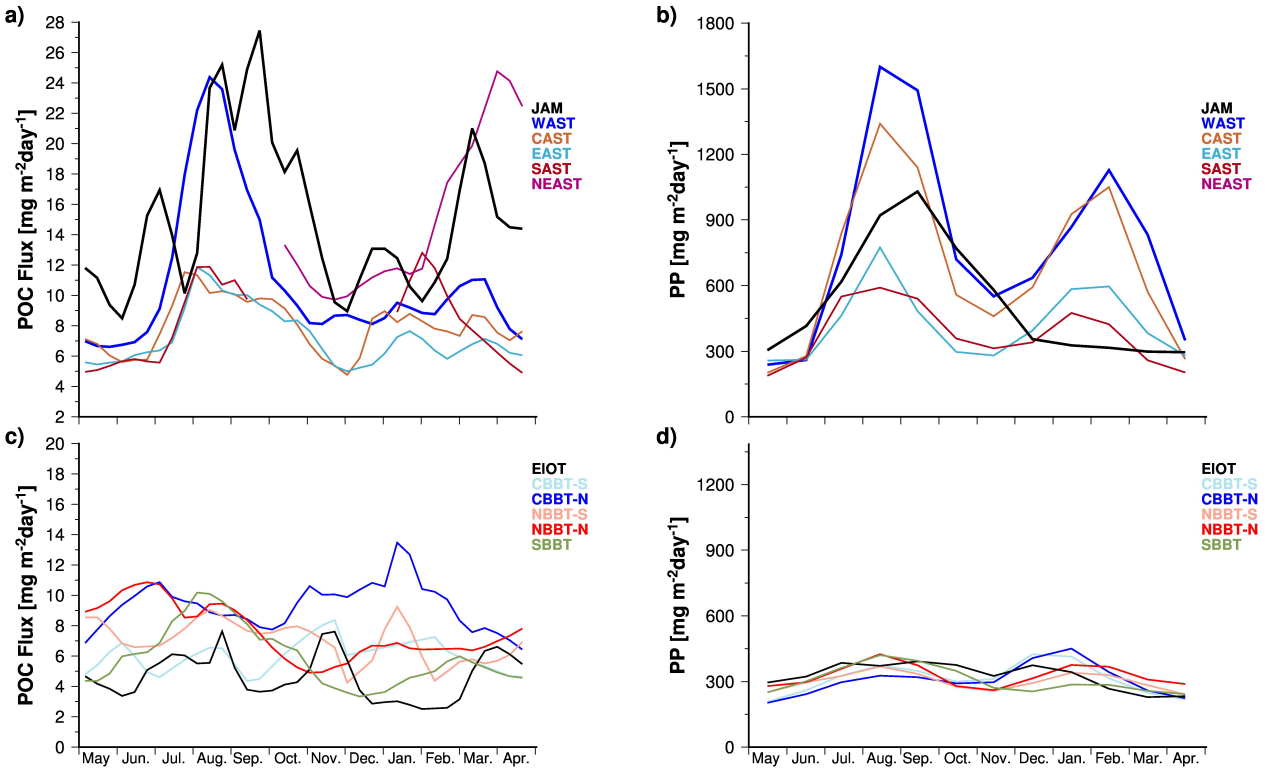
a)
POC Flux [mg m-2day-1]
JAM
WAST
CAST
EAST
SAST
NEAST
b)
PP [mg m-2day-1]
c)
EIOT
CBBT-S
CBBT-N
NBBT-S
NBBT-N
SBBT
d)
May
Jun.
Jul.
Aug.
Sep.
Oct.
Nov.
Dec.
Jan.
Feb.
Mar.
Apr.

5

Figure 4

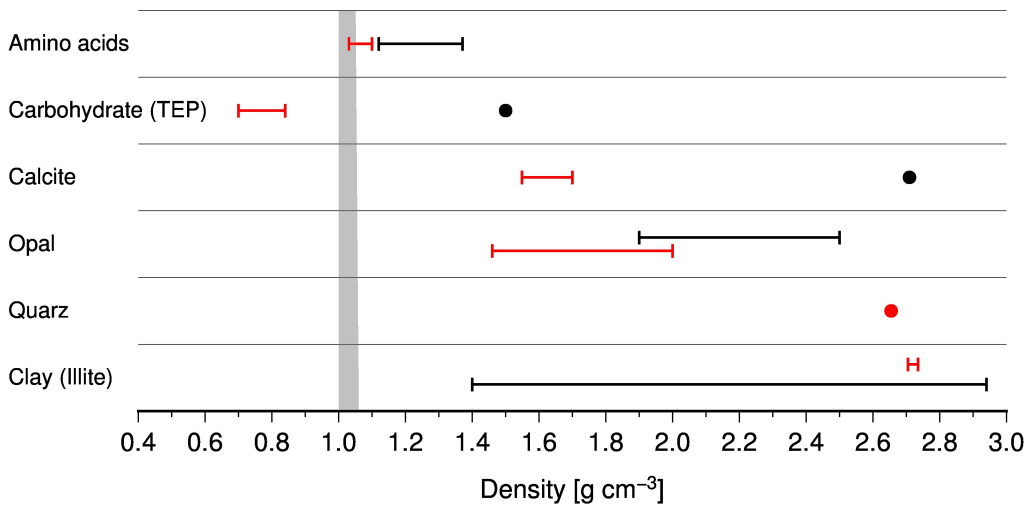
Amino acids
Carbohydrate (TEP)
Calcite
Opal
Quarz
Clay (Illite)
0.4
0.6
0.8
1.0
1.2
1.4
1.6
1.8
2.0
2.2
2.4
2.6
2.8
3.0
Density [g cm−3]

Figure 5

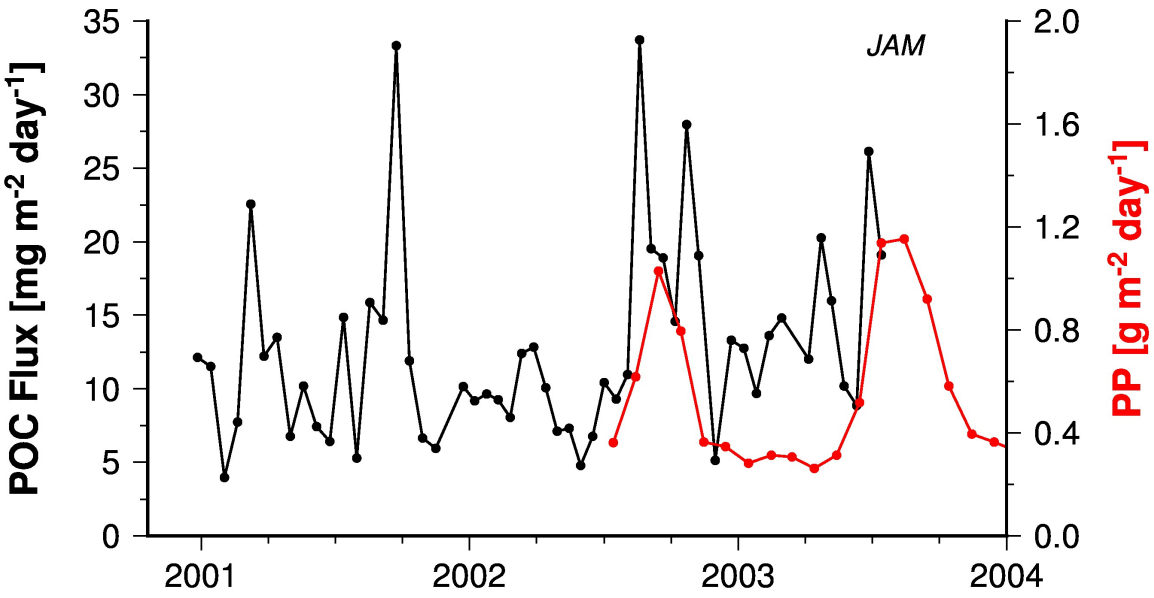
JAM
POC Flux [mg m-2 day-1]
PP [g m-2 day-1]
35
30
25
20
15
10
5
0
2.0
1.6
1.2
0.8
0.4
0.0
2001
2002
2003
2004

5

Figure 6

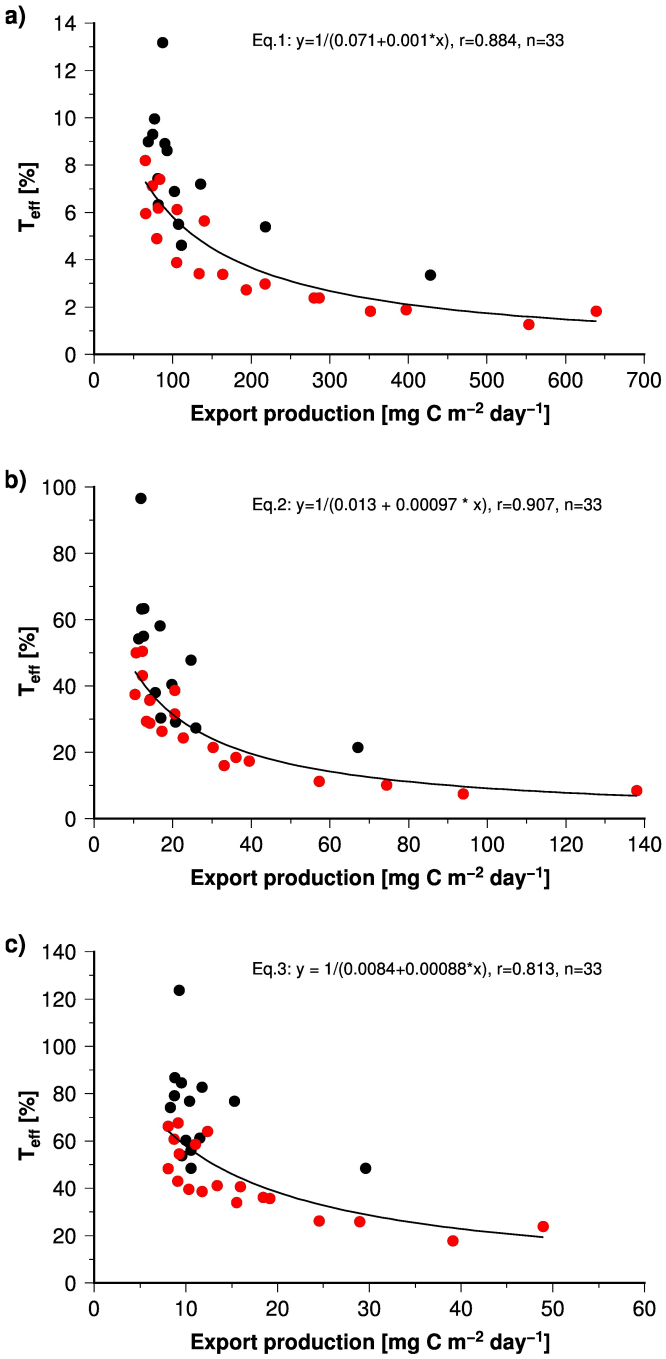
a)
Eq.1: y=1/(0.071+0.001*x), r=0.884, n=33
T_eff [%]
Export production [mg C m⁻² day⁻¹]
b)
Eq.2: y=1/(0.013 + 0.00097 * x), r=0.907, n=33
T_eff [%]
Export production [mg C m⁻² day⁻¹]
c)
Eq.3: y = 1/(0.0084+0.00088*x), r=0.813, n=33
T_eff [%]
Export production [mg C m⁻² day⁻¹]

Figure 7

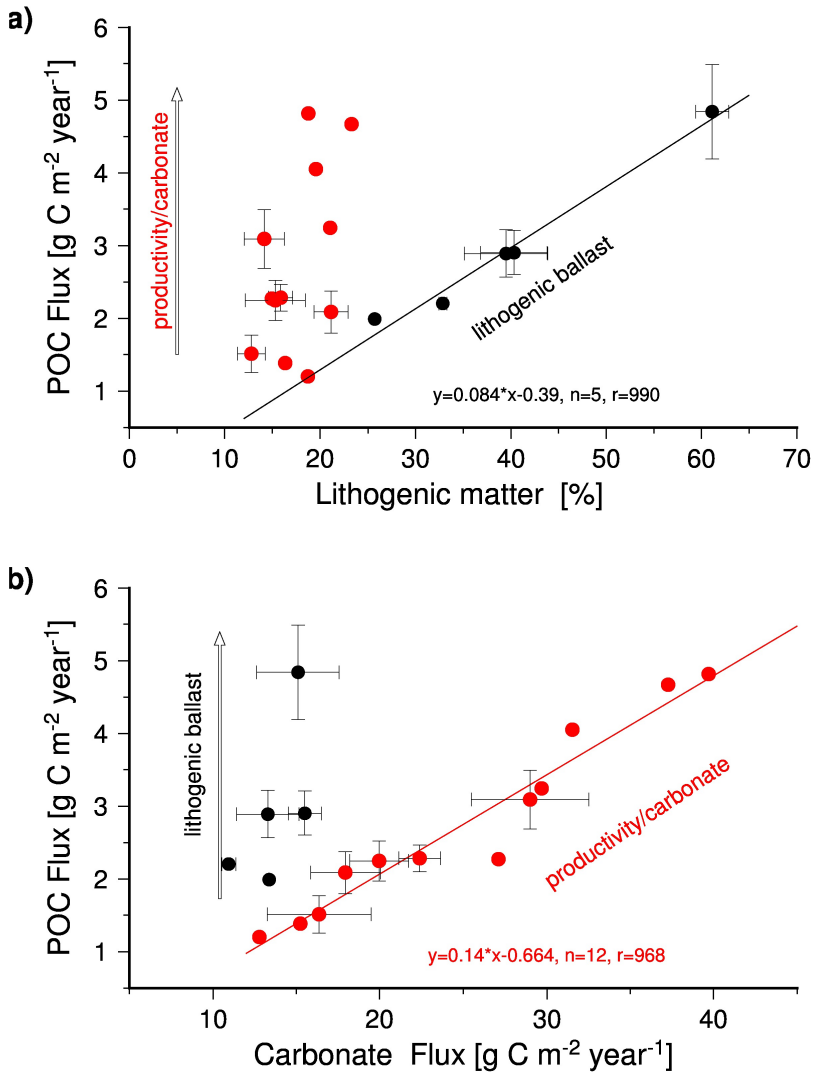
a)
POC Flux [g C m-2 year-1]
productivity/carbonate
lithogenic ballast
y=0.084*x-0.39, n=5, r=990
Lithogenic matter [%]
b)
POC Flux [g C m-2 year-1]
lithogenic ballast
productivity/carbonate
y=0.14*x-0.664, n=12, r=968
Carbonate Flux [g C m-2 year-1]

5

Figure 8

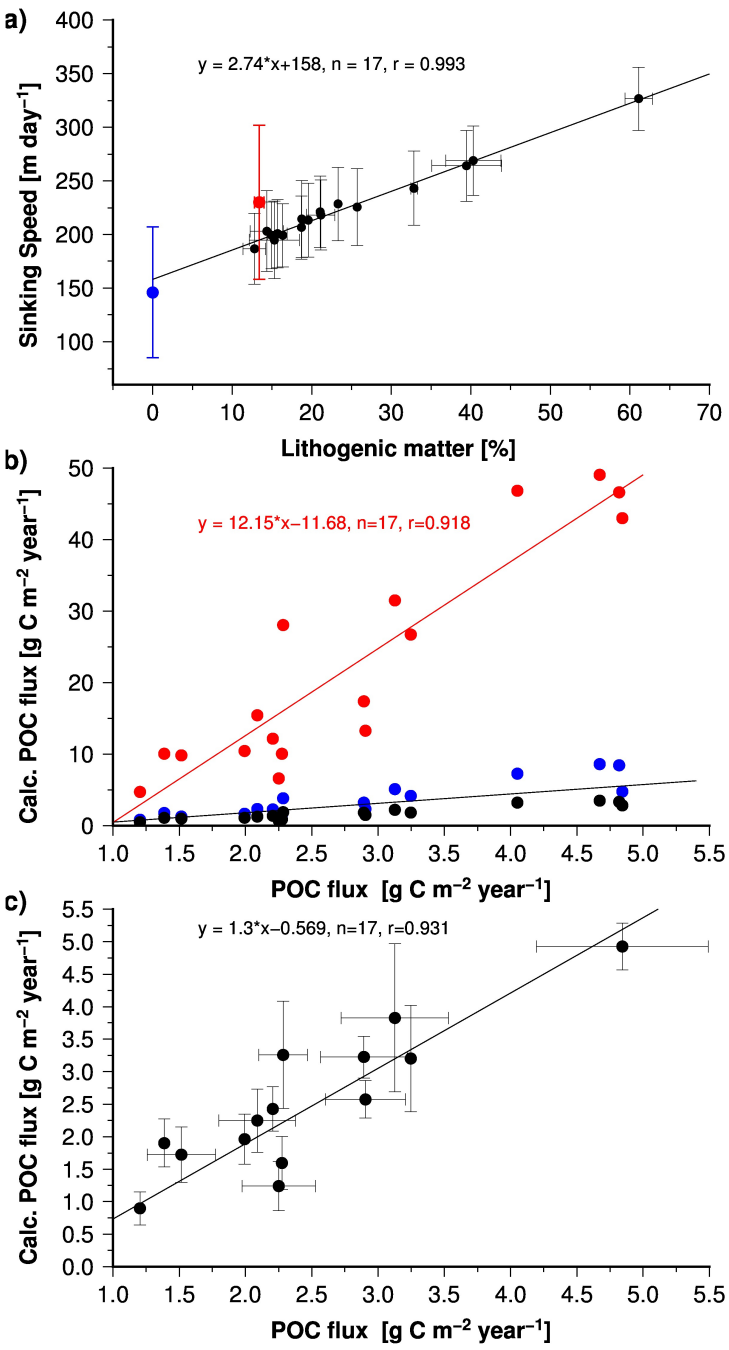
a)
y = 2.74*x+158, n = 17, r = 0.993
Sinking Speed [m day⁻¹]
Lithogenic matter [%]
b)
y = 12.15*x−11.68, n=17, r=0.918
Calc. POC flux [g C m⁻² year⁻¹]
POC flux [g C m⁻² year⁻¹]
c)
y = 1.3*x−0.569, n=17, r=0.931
Calc. POC flux [g C m⁻² year⁻¹]
POC flux [g C m⁻² year⁻¹]

Figure 9

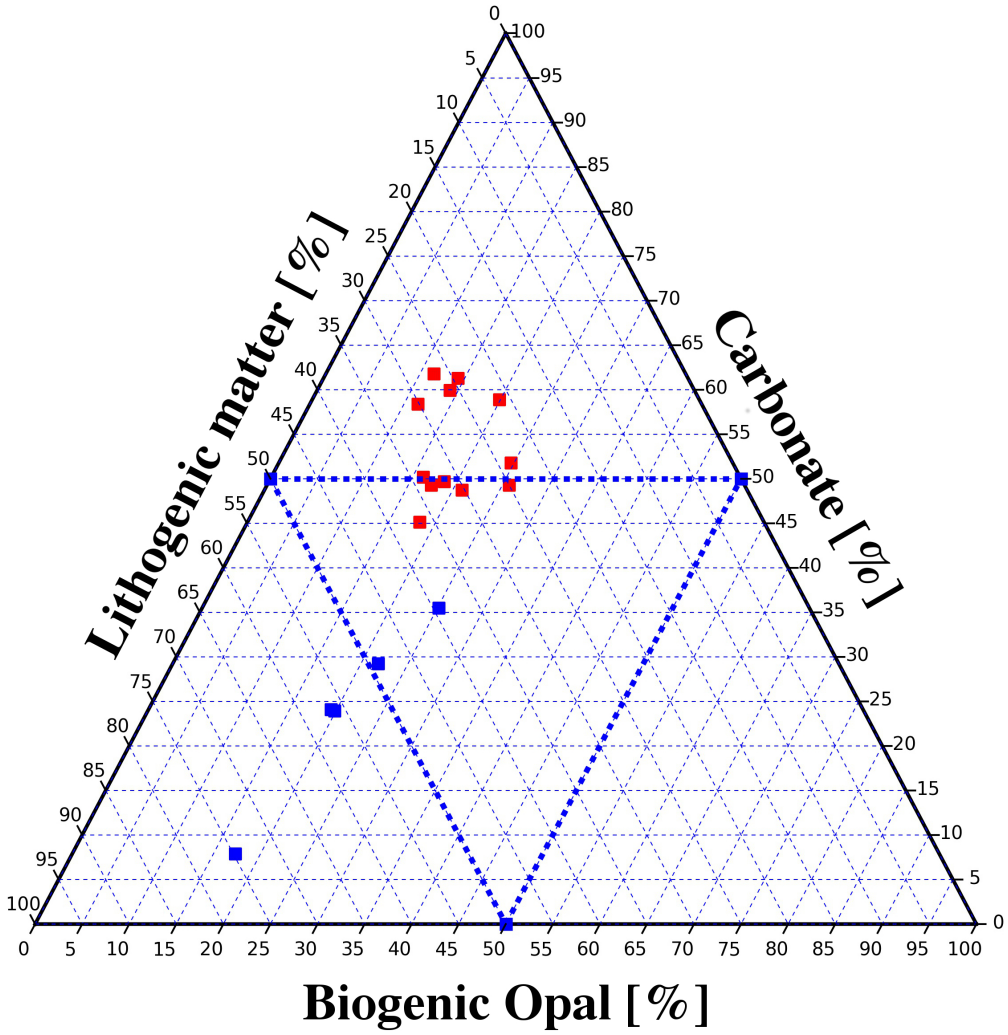

5